Dalton Transactions

PAPER

View Article Online
View Journal | View Issue

Cite this: *Dalton Trans.*, 2019, **48**, 3610

Catechol and 1,2,4,5-tetrahydroxybenzene functionalized cyclodiphosphazane ligands: synthesis, structural studies, and transition metal complexes†‡

Madhusudan K. Pandey,§[a] Harish S. Kunchur,§[a] Guddekoppa S. Ananthnag,¶§[a] Joel T. Mague[b] and Maravanji S. Balakrishna *[a]

Received 6th December 2018,
Accepted 23rd January 2019

DOI: 10.1039/c8dt04819c

rsc.li/dalton

Syntheses of two novel cyclodiphosphazane derivatives appended on catechol and 1,2,4,5-tetrahydroxy benzene, [{(μ-N(^{t}Bu)P)$_2$(C$_6$H$_4$O$_2$)}] (**1**) and [{((μ-N(^{t}Bu)P)$_2$)$_2$(μ-C$_6$H$_2$O$_4$)}] (**2**), are described. Reactions of **1** with copper(I) halides led to the isolation of one-dimensional (1-D) and two-dimensional (2-D) coordination polymers, depending on the reaction conditions, metal-to-ligand ratio and CuX (X = Cl, Br or I) employed. The 1 : 1 reaction between **1** and CuCl yielded a 1-D coordination polymer [{(μ-N(^{t}Bu)P)$_2$(C$_6$H$_4$O$_2$)}{Cu(μ$_2$-Cl)(NCCH$_3$)}$_2$]$_n$ (**3**) containing [Cu(μ$_2$-Cl)]$_2$ rhombus units. Similar reactions of **1** with CuBr and CuI produced rare 1-D coordination polymers [{(μ-N(^{t}Bu)P)$_2$(C$_6$H$_4$O$_2$)}{CuX(NCCH$_3$)}]$_n$ (**4**, X = Br; **5**, X = I) with discrete copper atoms linked by bridging cyclodiphosphazane ligands. However, the reactions of **1** with CuX (X = Cl, Br or I) in 1 : 2 molar ratios afforded 2-D coordination polymers [{(μ-N(^{t}Bu)P)$_2$(C$_6$H$_4$O$_2$)}$_2${Cu$_4$(μ$_3$-X)$_4$}]$_n$ (**6**, X = Cl; **7**, X = Br and **8**, X = I) containing cuboids [Cu$_4$(μ$_3$-X)$_4$] with **1** linking such units. Treatment of **1** with [RuCl$_2$(η^6-*p*-cymene)]$_2$, [Rh(COD)Cl]$_2$ and [Pd(η^3-C$_3$H$_5$)Cl]$_2$ in 1 : 1 molar ratios produced dinuclear complexes [{(μ-N(^{t}Bu)P)$_2$(C$_6$H$_4$O$_2$)}{RuCl$_2$(η^6-*p*-cymene)}$_2$] (**9**), [{(μ-N(^{t}Bu)P)$_2$(C$_6$H$_4$O$_2$)}{RhCl(COD)}$_2$] (**10**) and [{(μ-N(^{t}Bu)P)$_2$(C$_6$H$_4$O$_2$)}{PdCl(η^3-C$_3$H$_5$)}$_2$] (**11**), respectively. The reaction between **1** and [AuCl(SMe$_2$)] in a 1 : 2 ratio yielded a dinuclear complex [{(μ-N(^{t}Bu)P)$_2$(C$_6$H$_4$O$_2$)}{AuCl}$_2$] (**12**). The reactions of **2** with [RuCl$_2$(η^6-*p*-cymene)]$_2$, [Rh(COD)Cl]$_2$ and [Pd(η^3-C$_3$H$_5$)Cl]$_2$ in 1 : 2 molar ratios afforded tetranuclear complexes [{((μ-N(^{t}Bu)P)$_2$)$_2$(μ-C$_6$H$_2$O$_4$)}{RuCl$_2$(η^6-*p*-cymene)}$_4$] (**13**), [{((μ-N(^{t}Bu)P)$_2$)$_2$(μ-C$_6$H$_2$O$_4$)}{RhCl(COD)}$_4$] (**14**) and [{((μ-N(^{t}Bu)P)$_2$)$_2$(μ-C$_6$H$_2$O$_4$)}{PdCl(η^3-C$_3$H$_5$)}$_4$] (**15**), respectively. The reaction of **2** with [AuCl(SMe$_2$)] also afforded a tetranuclear complex [{((μ-N(^{t}Bu)P)$_2$)$_2$(μ-C$_6$H$_2$O$_4$)}{AuCl}$_4$] (**16**). In all these complexes, ligands preferred a bridged bidentate mode of coordination. Compounds **3–8** are the rare examples of 1-D and 2-D copper(I) coordination polymers containing cyclodiphosphazane ligands. The crystal structures of **2–8**, and **15** were established by X-ray diffraction studies.

Introduction

Cyclodiphosphazanes or diazadiphosphetidines of the general type [XP(μ-NR)]$_2$ (R = alkyl, aryl; X = halo, alkoxy) are saturated four-membered inorganic rings containing alternate phosphorus and nitrogen atoms. These nearly planar rings exist in *cis*- and *trans*-isomeric forms with respect to the exocyclic-phosphorus substituents with a small energy difference, and in the solid state, they prefer the thermodynamically stable *cis*-conformation.[1–7] *cis*-Orientation of the phosphorus lone pairs and rigidity of the planar four-membered ring make them valuable compounds in anion recognition study,[8,9] biradicaloid[10–15] and supramolecular chemistry.[16–21] Utility of these compounds as neutral ligands for the construction of polynuclear metalomacrocycles,[22–25] inorganic rings,[18,26–40]

[a]*Phosphorus Laboratory, Department of Chemistry, Indian Institute of Technology Bombay, Powai, Mumbai, 400076, India. E-mail: krishna@chem.iitb.ac.in, msb_krishna@iitb.ac.in; Fax: +91-22-5172-3480/2576-7152*

[b]*Department of Chemistry, Tulane University, New Orleans, Louisiana, 70118, USA*

† Dedicated to Main Group Chemist Prof. Tristram Chivers.

‡ Electronic supplementary information (ESI) available: NMR and HRMS data for **1–16**; crystallographic information for compounds **2–8** and **15**. CCDC 1883215–1883222. For ESI and crystallographic data in CIF or other electronic format see DOI: 10.1039/c8dt04819c

§ These authors contributed equally to this work.

¶ Present address: Department of Chemistry, BMS College of Engineering, Bull Temple Road, Bengaluru 560019, India.

and 1-D,[41–44] 2-D,[45] and 3-D[43,46] coordination polymers is well documented. The recent trend is to synthesize these main group compounds using mechanochemical methods.[40,47,48] The copper(I) complexes of cyclodiphosphazanes have been extensively studied by our group.[1,22–24,41,42,49] The structural features of the resulting complexes formed are highly dependent on the nature of phosphorus substituents, stoichiometry of the reagents and reaction conditions, especially in the reactions of cyclodiphosphazanes with copper(I) halides. Further, copper(I) halides can also display a wide range of structures (**I–VI**) when coordinated to cyclodiphosphazanes (Chart 1).[1] The geometry adopted by copper(I) is generally trigonal planar or tetrahedral, depending upon the availability of other donor atoms besides the phosphorus atoms of cyclodiphosphazane or the presence of coordinating solvents. The steric and electronic attributes of phosphorus and nitrogen substituents also play a key role in their ligating ability. In general, cyclodiphosphazanes can form simple mono- (**I**) or bimetallic (**II–VI**) complexes. The monodentate coordination leads to mononuclear species **I**,[41] whereas the bridged bidentate mode can produce cyclic (**II**)[45] or polymeric structures (**III–VI**) (Chart 1).[41,43,45,46] In our efforts to identify rigid 2-D and 3-D coordination polymers of soft metal ions and soft ligands with desired cavities to explore in catalytic and sensing applications, we have sought to prepare multidentate phosphorus donor systems with a rigid ligand framework to facilitate the formation of 2- or 3-dimensional coordination polymers. Herein, we report the synthesis of two novel cyclodiphosphazane derivatives and their transition metal chemistry.

Results and discussion

Synthesis of [{(μ-N(^{t}Bu)P)$_2$($C_6H_4O_2$)}] (1) and [{((μ-N(^{t}Bu)P)$_2$)$_2$(μ-$C_6H_2O_4$)}] (2)

The reaction of catechol with one equivalent of *cis*-[ClP(μ-N^{t}Bu)]$_2$ in the presence of triethylamine afforded [{(μ-N(^{t}Bu)P)$_2$($C_6H_4O_2$)}] (**1**) as a white solid. A similar reaction of 1,2,4,5-tetrahydroxybenzene with two equivalents of *cis*-[ClP(μ-N^{t}Bu)]$_2$ afforded [{((μ-N(^{t}Bu)P)$_2$)$_2$(μ-$C_6H_2O_4$)}] (**2**) as shown in Scheme 1. Compound **1** is a low melting solid (73–76 °C), whereas **2** melts at higher temperatures (198–203 °C). The $^{31}P\{^1H\}$ NMR spectra of **1** and **2** consisted of single resonances around 180 ppm, which are slightly shielded compared to those of the parent compound *cis*-[ClP(μ-N^{t}Bu)]$_2$ (δP 207).[26] In the ^{1}H NMR spectra of **1** and **2**, the ^{t}Bu protons appeared as singlets around 1.10 ppm. In the $^{13}C\{^1H\}$ NMR spectra of **1** and **2**, the quaternary carbons of ^{t}Bu groups showed triplets around 51.4 ppm with $^2J_{PC}$ couplings of 7.1 and 6.7 Hz, respectively. The aliphatic carbons of ^{t}Bu groups also showed

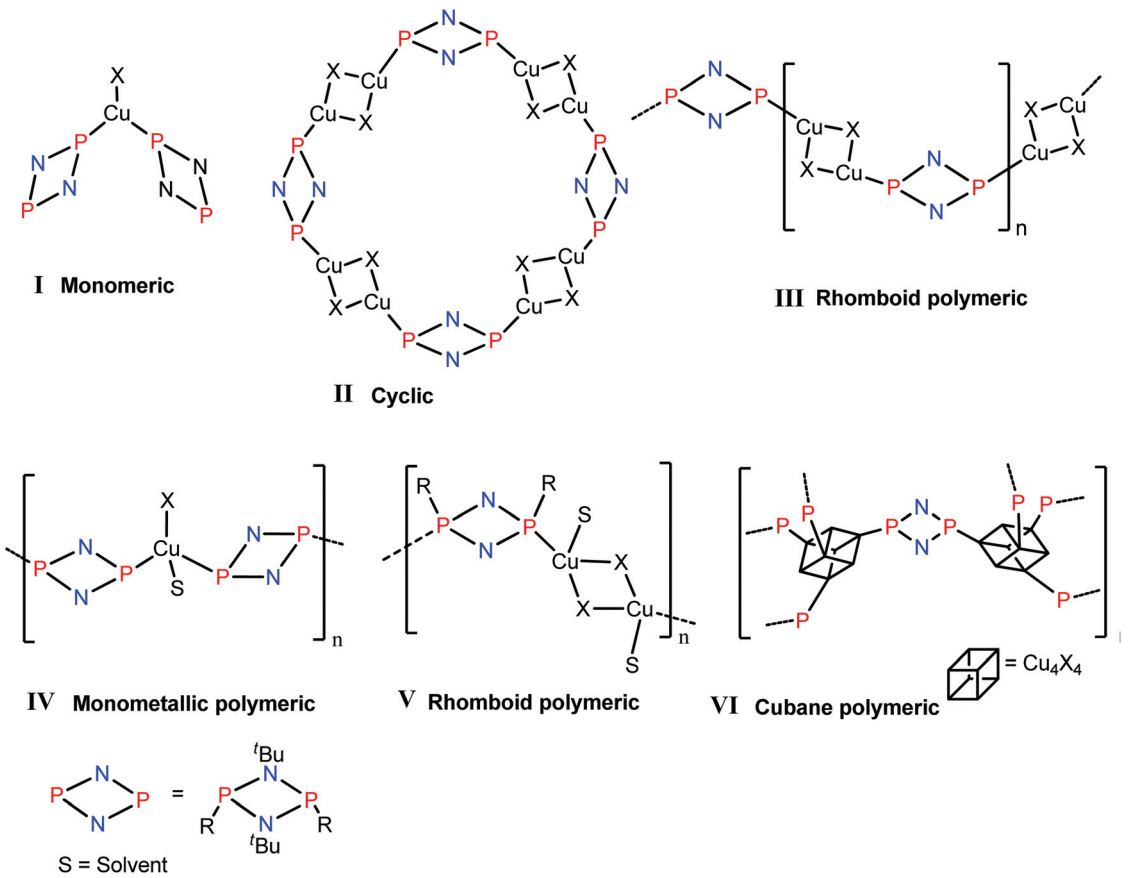

Chart 1 Possible structural motifs for copper(I) complexes of cyclodiphosphazane.

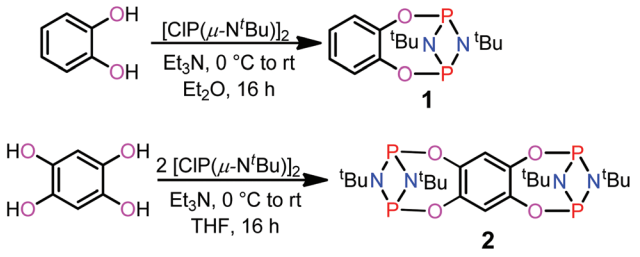

Scheme 1 Synthesis of **1** and **2**.

triplets around 30.4 ppm with a $^{3}J_{PC}$ coupling of 5.6 Hz. HRMS spectra showed molecular ion peaks $(M + H)^{+}$ at 313.1229 and $[M + H]^{+}$ at 547.1913 for **1** and **2**, respectively. The molecular structure of **2** was confirmed by X-ray diffraction analysis.

Molecular structure of [{((μ-N(ᵗBu)P)$_2$)$_2$(μ-C$_6$H$_2$O$_4$)}] (2)

The perspective view of the molecular structure of **2** along with the selected bond parameters is shown in Fig. 1. The crystallographic data and the details of the structure determination are given in Table 5. In the molecular structure of **2**, the central benzene ring, four oxygen and four P atoms are coplanar and the N_2P_2 rings are orthogonal to this plane. The average P–N bond distance of 1.700(2) Å in **2** is similar to that found in *N*-(2,6-dibenzhydryl-4-methylphenyl)diphenylphosphinamine 1.702(13) Å,[50] but is slightly shorter than those observed in [Fe(η^5-C$_5$H$_4$)$_2${μ-N(ᵗBu)P}$_2$] (1.741(1) and 1.736(1) Å)[51] and longer than that in 2,6-{μ-(N^{t}Bu)$_2$P(^{t}BuNH)PO}$_2$C$_6$H$_3$I (1.666(3)–1.686(3) Å).[52] The P–O bond distances of 1.6501(19) and 1.6565(19) Å in **2** are similar to that found in [(4-CN-PhO)P(μ-N^{t}Bu)]$_2$ (1.658(1)–1.678(1) Å).[53]

Synthesis of 1-D and 2-D coordination polymers of copper(I)

The reactions of [{(μ-N(ᵗBu)P)$_2$(C$_6$H$_4$O$_2$)}] (**1**) with CuX (X = Cl, Br and I) in 1 : 1 and 1 : 2 molar ratios afforded [{(μ-N(ᵗBu)P)$_2$(C$_6$H$_4$O$_2$)}{Cu(μ$_2$-Cl)(NCCH$_3$)}$_2$]$_n$ (**3**), [{(μ-N(ᵗBu)P)$_2$(C$_6$H$_4$O$_2$)}{CuX(NCCH$_3$)}]$_n$ (**4**, X = Br; **5**, X = I) as 1-D and [{(μ-N(ᵗBu)P)$_2$(C$_6$H$_4$O$_2$)}$_2${Cu$_4$(μ$_3$-X)$_4$}]$_n$ (**6**, X = Cl; **7**, X = Br; **8**, X = I) 2-D coordination polymers, respectively. Similar reactions of [{((μ-N(ᵗBu)P)$_2$)$_2$(μ-C$_6$H$_2$O$_4$)}] (**2**) with CuX afforded highly insoluble compounds, and attempts to crystallize them have been unsuccessful. The reactions of **1** with CuX (X = Cl, Br or I) in 1 : 1 molar ratios in dichloromethane/acetonitrile (1 : 1 v/v) afforded two types of 1-D coordination polymers. The chloro-derivative [{(μ-N(ᵗBu)P)$_2$(C$_6$H$_4$O$_2$)}{Cu(μ$_2$-Cl)(NCCH$_3$)}$_2$]$_n$ (**3**) consisted of rhombic [Cu(μ$_2$-Cl)]$_2$ and N_2P_2 moieties as repeating units, whereas the coordination polymers of CuBr and CuI [{(μ-N(ᵗBu)P)$_2$(C$_6$H$_4$O$_2$)}{CuX(NCCH$_3$)}]$_n$ (**4**, X = Br; **5**, X = I) preferred tetracoordinated copper(I) linkers as shown in Scheme 2. These complexes were precipitated from the reaction mixture as insoluble white solids. The poor solubility of **3–5** in most of the organic solvents prevented the NMR studies. However, X-ray quality crystals of **3–5** were grown by the slow diffusion of acetonitrile solution of CuX into the dichloromethane solution of **1**. The phase purity of the bulk material was confirmed by powder X-ray diffraction analysis (see ESI Fig. S9–S11‡).

Molecular structures of **3–5** were established from single-crystal X-ray diffraction analyses (Fig. 2). The structure of **3** consists of [Cu(μ$_2$-Cl)]$_2$ units coordinated on both the ends by N_2P_2 rings to form a one-dimensional chain, and one of the coordination sites on each copper is occupied by an acetonitrile molecule. In the molecular structures of **4** and **5**, each copper atom is coordinated to two molecules of **1**, one halide

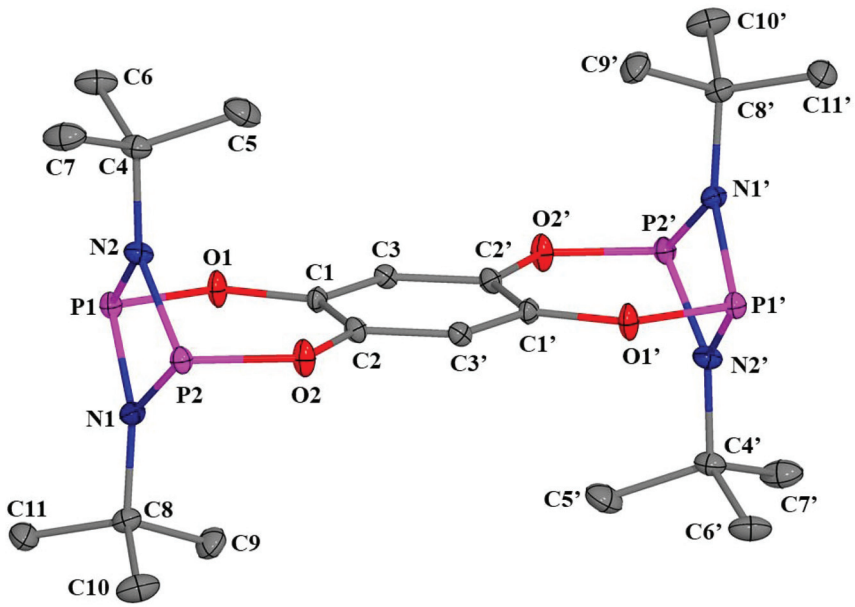

Fig. 1 Molecular structure of [{((μ-N(ᵗBu)P)$_2$)$_2$(μ-C$_6$H$_2$O$_4$)}] (**2**). Thermal ellipsoids are drawn at the 30% probability level. All hydrogen atoms have been omitted for the sake of clarity. Selected bond lengths (Å) and bond angles (°): P1–N1 1.703(2), P1–N2 1.700(2), P1–O1 1.6565(19), P2–O2 1.6501(19), O2–P2–P1 100.87(7), O2–P2–N1 103.27(11), O2–P2–N2 103.22(11), N2–P2–N1 81.22(11), N2–P1–N1 81.35(11).

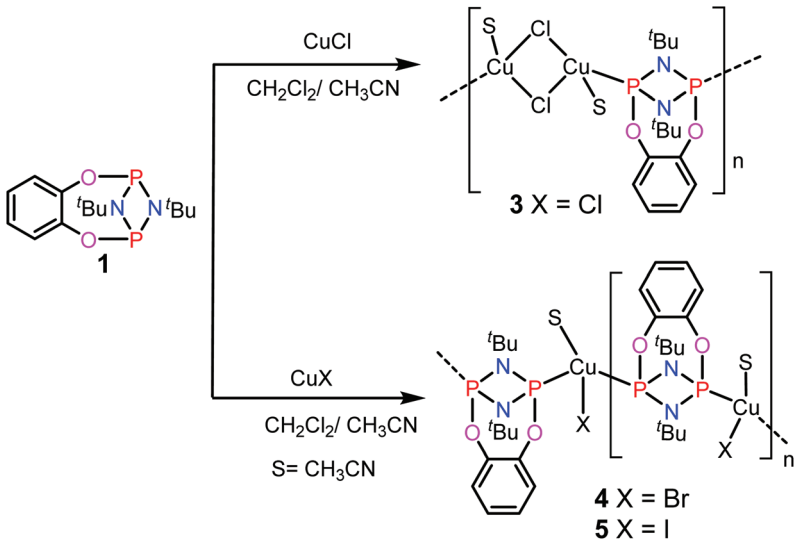

Scheme 2 Synthesis of 1-D coordination polymers **3–5**.

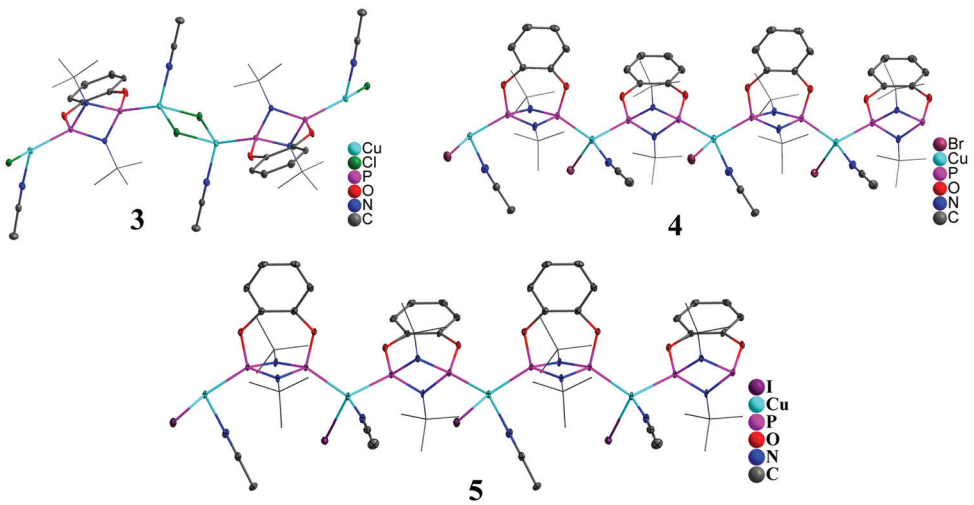

Fig. 2 The molecular structures of $[\{(\mu\text{-N}(^t\text{Bu})\text{P})_2(C_6H_4O_2)\}\{Cu(\mu_2\text{-Cl})(NCCH_3)\}_2]_n$ (**3**) and $[\{(\mu\text{-N}(^t\text{Bu})\text{P})_2(C_6H_4O_2)\}\{CuX(NCCH_3)\}]_n$ (**4**, X = Br; **5**, X = I). All hydrogen atoms have been omitted for clarity. Thermal ellipsoids are drawn at the 50% probability level.

ion (Br or I), and one acetonitrile molecule. The P_2N_2 core in **3** is puckered with an angle of 171.82°, and the nitrogen atoms are deviated by 0.086 Å from the mean plane. Similarly, in complexes **4** and **5**, the P_2N_2 core is puckered with angles of 173.5°, and the nitrogen atoms are deviated by 0.072 Å from the mean plane in both the cases. The $[Cu(\mu_2\text{-Cl})]_2$ units in **3** adopt a parallelogram configuration with an average Cu···Cu distance of 3.25 Å.[44,45] The average Cu···Cu, Cu–P and Cu–Cl bond distances in **3** are 3.25, 3.18 and 2.38 Å, respectively. The P–N, Cu–P and Cu–X bond distances in **3–5** are unexceptional and found to be in the same range reported for similar complexes.[43–45]

Synthesis of 2-D coordination polymers (6–8) of copper(I)

The reactions of $[\{(\mu\text{-N}(^t\text{Bu})\text{P})_2(C_6H_4O_2)\}]$ (**1**) and CuX (X = Cl, Br, I) in 1 : 2 molar ratios in a mixture of dichloromethane and acetonitrile afforded 2-D coordination polymers, $[\{(\mu\text{-N}(^t\text{Bu})\text{P})_2(C_6H_4O_2)\}_2\{Cu_4(\mu_3\text{-X})_4\}]_n$ (**6**, X = Cl; **7**, X = Br; **8**, X = I) containing $[Cu_4(\mu_3\text{-X})_4]$ cubanes and bridging N_2P_2 rings as the repeating units as shown in Scheme 3. Compounds **6–8** are insoluble in most of the organic solvents, but partially soluble in hot dimethyl sulfoxide (DMSO-d_6). The $^{31}P\{^1H\}$ NMR spectra of **6–8** in DMSO-d_6 showed broad singlets at 122.5, 120.3 and 125.2 ppm, respectively. The molecular structures of **6–8** were confirmed by single-crystal X-ray analyses. X-ray quality crystals of **6–8** were grown by the slow diffusion of acetonitrile solution of CuX into the dichloromethane solution of **1**. The phase purity of **6–8** was confirmed by powder X-ray diffraction analyses (see ESI Fig. S14, S17 and S20‡).

The perspective views of molecular structures of **6–8** along with the atom labelling schemes are shown in Fig. 3–5. All

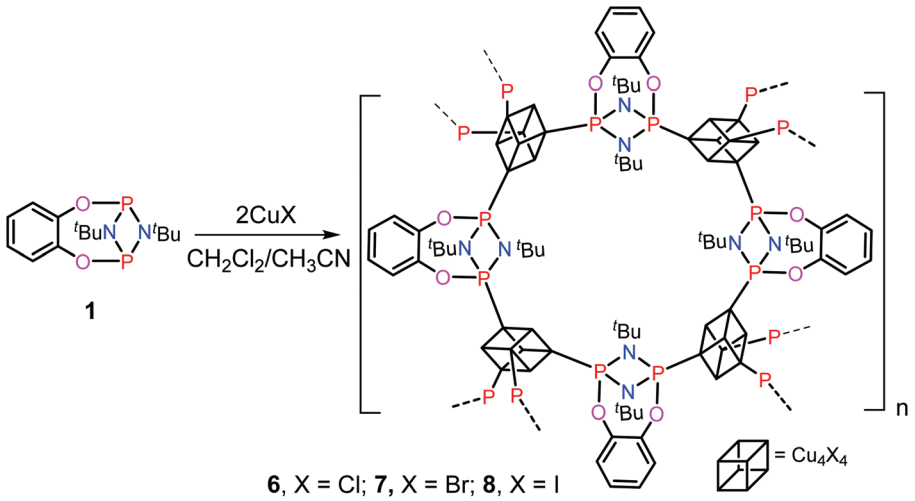

Scheme 3 Synthesis of 2-D coordination polymers **6–8**.

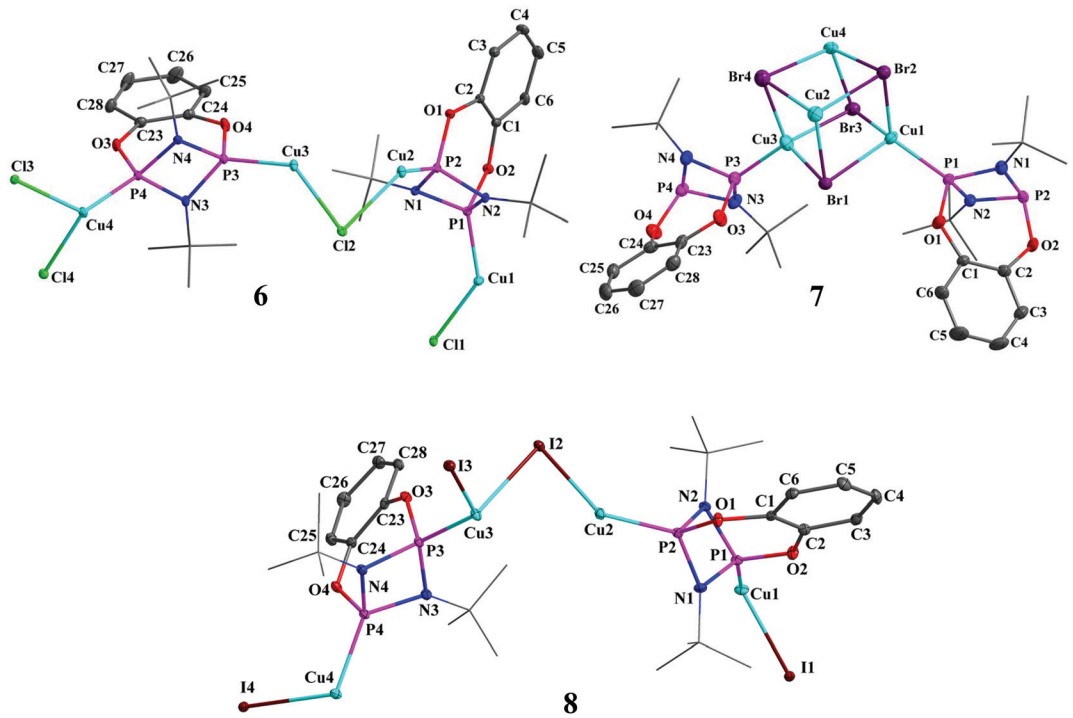

Fig. 3 The asymmetric unit of 2-D coordination polymers $[\{(\mu\text{-N}(^t\text{Bu})\text{P})_2(C_6H_4O_2)\}_2\{Cu_4(\mu_3\text{-X})_4\}]_n$ [(**6**, X = Cl; **7**, X = Br; **8**, X = I)] (**6–8**). All hydrogen atoms have been omitted for clarity.

these complexes have similar bond parameters. The fundamental building unit of **6–8** comprises two cyclodiphosphazane rings, four copper atoms and four halide ions, but with a slight difference in their arrangements in respective asymmetric units. In the asymmetric units of **6** and **8**, two ligands bridge four copper atoms *via* (μ_3-X) [X = Cl (**6**), I (**8**)], resulting in the formation of 2-D coordination polymer, while in the case of **7**, the asymmetric unit is made up of one cuboid $[Cu_4(\mu_3\text{-Br})_4]$ acting as a tetrahedral node flanked between two mono-coordinated P_2N_2 rings with other phosphorus atoms being uncoordinated. Thus, the cuboid with two uncoordinated phosphorus atoms at both the ends acts as a ditopic linker to form a 2-D coordination polymer as depicted in Fig. 4. The overall 2-D framework is made up of $[Cu_4(\mu_3\text{-X})_4]$ tetrahedral units with all four copper atoms coordinated by ditopic P_2N_2 linkers to form a "*shuttle net*" type network (Fig. 5). The Cu–P, P–N and Cu–X bond distances in **6–8** are unexceptional and found to be in the same range reported for similar complexes.[41,43,45,46]

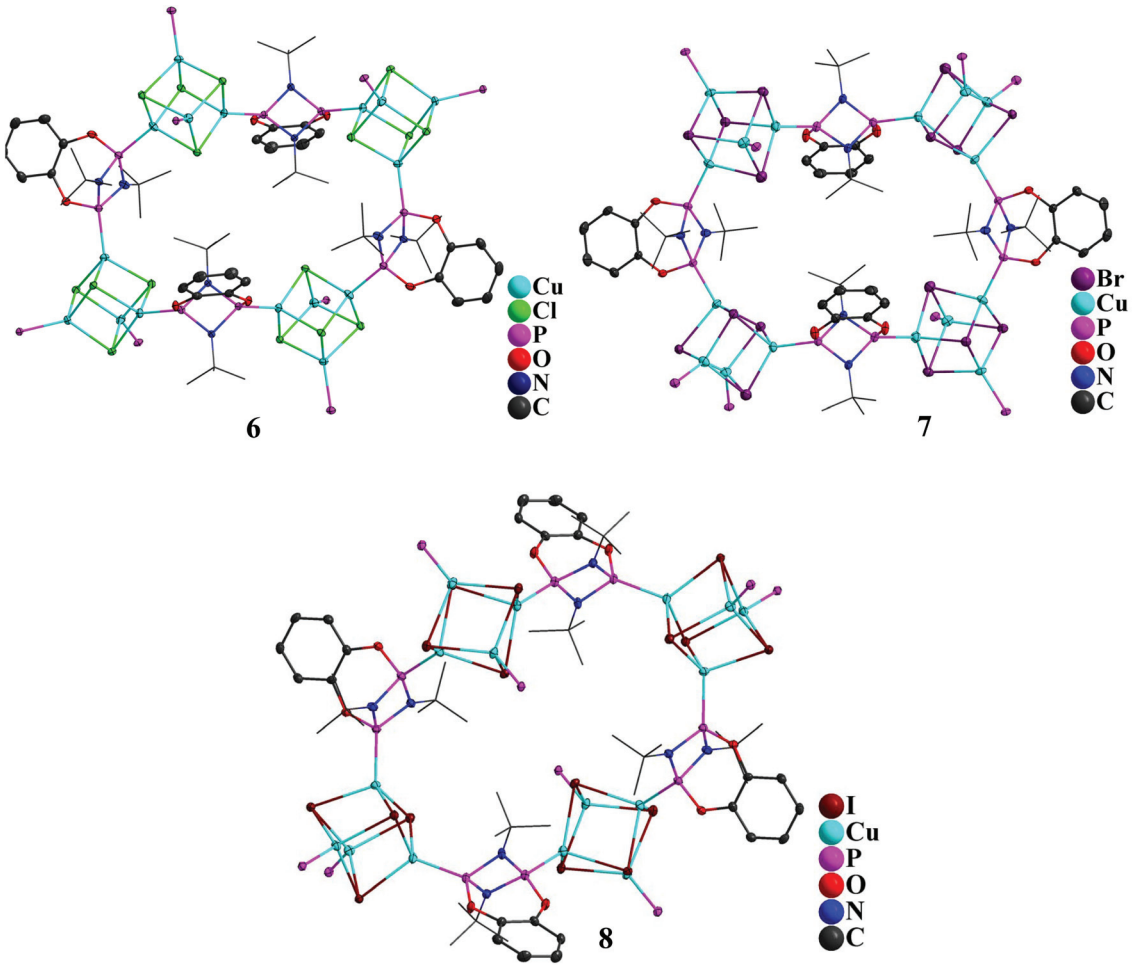

Fig. 4 Tetrameric repeating units of 2-D coordination polymers $[\{(\mu\text{-}N(^{t}Bu)P)_2(C_6H_4O_2)\}_2\{Cu_4(\mu_3\text{-}X)_4\}]_n$ [(**6**, X = Cl; **7**, X = Br; **8**, X = I)]. All hydrogen atoms have been omitted for clarity.

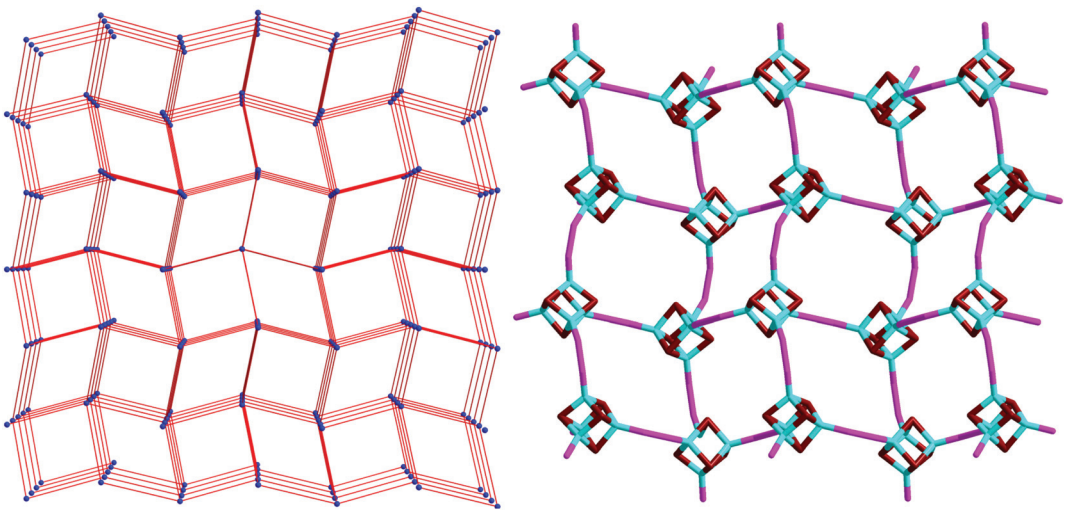

Fig. 5 Top view of one of the 2-D coordination polymers $[\{(\mu\text{-}N(^{t}Bu)P)_2(C_6H_4O_2)\}_2\{Cu_4(\mu_3\text{-}X)_4\}]_n$ [(**6**, X = Cl; **7**, X = Br; **8**, X = I)], showing "*shuttle net*" type structure. The *tert*-butyl group and catechol rings have been omitted for clarity.

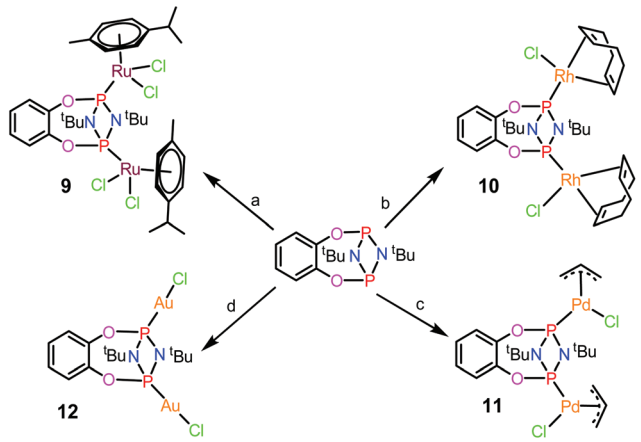

Scheme 4 Synthesis of Ru^{II}, Rh^{I}, Pd^{II} and Au^{I} complexes of **1**. Reaction conditions: (a) $[Ru(\eta^6\text{-}p\text{-cymene})Cl_2]_2$, CH_2Cl_2, rt, 5 h; (b) $[Rh(COD)Cl]_2$, CH_2Cl_2, rt, 5 h; (c) $[Pd(\eta^3\text{-}C_3H_5)Cl]_2$, CH_2Cl_2, rt, 5 h; (d) $[AuCl(SMe_2)]$, CH_2Cl_2, rt, 5 h.

Treatment of **1** with $[RuCl_2(\eta^6\text{-}p\text{-cymene})]_2$, $[Rh(COD)Cl]_2$, or $[Pd(\eta^3\text{-}C_3H_5)Cl]_2$ in 1 : 1 molar ratios in CH_2Cl_2 resulted in the formation of corresponding dinuclear complexes **9–11** in good yields as shown in Scheme 4. The $^{31}P\{^1H\}$ NMR spectrum of $[\{(\mu\text{-}N(^tBu)P)_2(C_6H_4O_2)\}\{RuCl_2(\eta^6\text{-}p\text{-cymene})\}_2]$ (**9**) showed a doublet of doublets centered at 140.4 and 127.8 ppm, with a $^2J_{PP}$ coupling of 45.4 Hz, indicating the presence of two non-equivalent phosphorus atoms. In the ^1H NMR spectrum of **9**, a singlet was observed at 1.42 ppm due to the ^tBu protons, whereas aromatic protons displayed multiplets in the range of 7.15–7.33 ppm. The aromatic protons of the *p*-cymene group appeared as multiplets at 5.39 and 5.69 ppm. Methyl protons of the isopropyl group appeared as a doublet at 1.36 ppm, whereas the methyl protons of *p*-cymene showed two singlets at 2.33 and 2.43 ppm. The $^{31}P\{^1H\}$ NMR spectrum of $[\{(\mu\text{-}N(^tBu)P)_2(C_6H_4O_2)\}\{RhCl(COD)\}_2]$ (**10**) showed two doublet of doublets centered at 124.7 and 124. 2 ppm with the following couplings: ($^1J_{RhP}$ = 246.9 and 240.9 Hz, and $^2J_{PP}$ = 27.2 Hz). In contrast, the $^{31}P\{^1H\}$ NMR spectrum of $[\{(\mu\text{-}N(^tBu)P)_2(C_6H_4O_2)\}\{PdCl(\eta^3\text{-}C_3H_5)\}_2]$ (**11**) showed a single resonance at 135.2 ppm, indicating the symmetrical nature of all phosphorus atoms. The reaction of **1** with two equivalents of $[AuCl(SMe_2)]$ in CH_2Cl_2 resulted in $[\{(\mu\text{-}N(^tBu)P)_2(C_6H_4O_2)\}\{AuCl\}_2]$ (**12**) as a white solid (Scheme 4). The $^{31}P\{^1H\}$ NMR spectrum of **12** showed a single resonance at 117 ppm. The ^1H NMR data and mass spectrometry supported the product formation in all cases. The microanalysis data are also consistent with the proposed structures.

Treatment of **2** with $[RuCl_2(\eta^6\text{-}p\text{-cymene})]_2$, $[Rh(COD)Cl]_2$, or $[Pd(\eta^3\text{-}C_3H_5)Cl]_2$ in 1 : 2 molar ratios afforded corresponding tetranuclear complexes **13–15** as shown in Scheme 5. The $^{31}P\{^1H\}$ NMR spectrum of $[\{((\mu\text{-}N(^tBu)P)_2)_2(\mu\text{-}C_6H_2O_4)\}\{RuCl_2(\eta^6\text{-}p\text{-cymene})\}_4]$ (**13**) showed a doublet of doublets centered at 142.3 and 129.6 ppm, with a $^2J_{PP}$ coupling of 44.5 Hz, suggesting the asymmetrical nature of the coordinated phosphorus atoms. Similarly, the ^1H NMR spectrum of **13** showed singlets at 1.44 and 7.30 ppm due to ^tBu and aromatic protons, respectively. The $^{31}P\{^1H\}$ NMR spectrum of $[\{((\mu\text{-}N(^tBu)P)_2)_2(\mu\text{-}C_6H_2O_4)\}\{RhCl(COD)\}_4]$ (**14**) showed two doublet of doublets centered at 125.5 and 124.9 ppm with $^1J_{RhP}$ couplings of 246.9 and 242.8 Hz with a $^2J_{PP}$ coupling of 26.8 Hz, indicating the presence of magnetically non-equivalent phosphorus atoms in **14**. The $^{31}P\{^1H\}$ NMR spectrum of complex $[\{((\mu\text{-}N(^tBu)P)_2)_2(\mu\text{-}C_6H_2O_4)\}\{PdCl(\eta^3\text{-}C_3H_5)\}_4]$ (**15**) showed a single resonance at 137.4 ppm. The allylic group in square planar transition metal complexes is known to undergo η^3 to η^1 conversion influenced by the ligand steric attributes.[54,55] The presence of sterically bulky ^tBu groups in **15** retards the η^3 to η^1 conversion process as

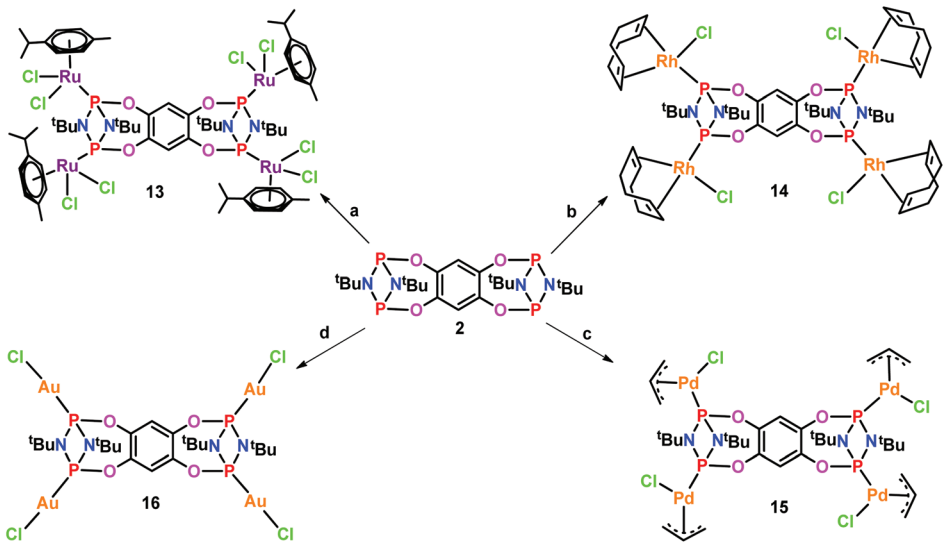

Scheme 5 Synthesis of Ru^{II}, Rh^{I}, Pd^{II} and Au^{I} complexes of **2**. Reaction conditions: (a) $[Ru(\eta^6\text{-}p\text{-cymene})Cl_2]_2$, CH_2Cl_2, rt, 5 h; (b) $[Rh(COD)Cl]_2$, CH_2Cl_2, rt, 5 h; (c) $[Pd(\eta^3\text{-}C_3H_5)Cl]_2$, CH_2Cl_2, rt, 5 h; (d) $[AuCl(SMe_2)]$, CH_2Cl_2, rt, 5 h.

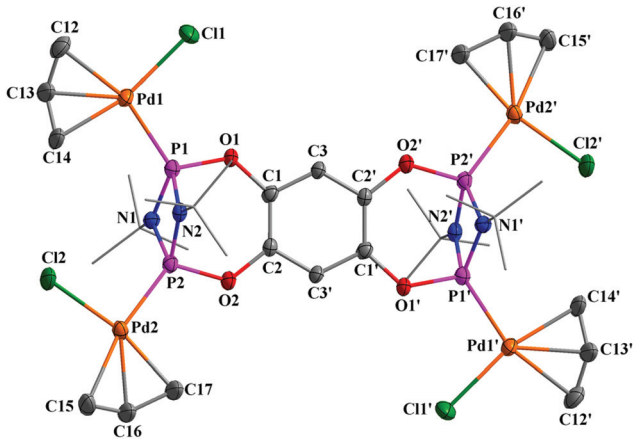

Fig. 6 Molecular structure of $[\{((\mu\text{-}N(^{t}Bu)P)_2)_2(\mu\text{-}C_6H_2O_4)\}\{PdCl(\eta^3\text{-}C_3H_5)\}_4]$ (**15**). Hydrogen atoms excluded for clarity.

evinced by the ^{1}H NMR spectral data. The allylic protons showed five distinct signals for each proton of the allyl group, ruling out the possibility of η^3 to η^1 transformation in solution. The reaction of **2** with four equivalents of $[AuCl(SMe_2)]$ in CH_2Cl_2 resulted in the formation of the tetragold complex $[\{((\mu\text{-}N(^{t}Bu)P)_2)_2(\mu\text{-}C_6H_2O_4)\}\{AuCl\}_4]$ (**16**) as a white solid (Scheme 5). The $^{31}P\{^1H\}$ NMR spectrum of **16** showed a single resonance at 120.5 ppm. The molecular structure of **15** was confirmed by single crystal X-ray analysis.

The perspective view of the molecular structure of **15** along with the atom labelling scheme is shown in Fig. 6. The yellow crystals of **15** suitable for the single crystal X-ray diffraction study were obtained by the solvent diffusion technique using dichloromethane and petroleum ether as solvents at room temperature. The geometry around the palladium center is distorted square planar with the following bond angles: (P1–Pd1–Cl1 = 100.40(10), C14–Pd1–P1 = 94.0(3) and C12–Pd1–Cl1 = 98.6(3)°). The average P–N and P–O bond distances (1.678 Å and 1.627 Å) are shorter those in the free ligand **2** (1.701 Å and 1.653 Å). The average Pd–P and Pd–Cl distances are 2.243 Å and 2.356 Å, respectively. The Pd–C (allyl), Pd–P and Pd–Cl bond lengths are typical for these types of complexes.[50,56]

Table 1 Selected bond lengths (Å) and bond angles (°) of compounds **3–5**

	3	4	5
Bond lengths (Å)			
Cu1–P1	2.1863(6)	2.2351(8)	2.2256(10)
Cu2–P2	2.1737(5)	2.2310(8)	2.2247(10)
Cu1–X1	2.3483(5)	2.4223(5)	2.5929(5)
Cu2–X2	2.3394(6)	2.4220(5)	2.6091(5)
P1–N1	1.6932(17)	1.691(3)	1.687(3)
P1–N2	1.6978(17)	1.686(3)	1.682(3)
Bond angles (°)			
Cu1–P1–N1	127.17(6)	123.27(19)	121.38(11)
Cu2–P2–N2	128.70(6)	123.51(9)	123.11(11)
X2–Cu2–P2	128.40(2)	99.13(2)	98.95(3)
X1–Cu1–P1	132.07(2)	114.57(3)	115.54(3)

Table 2 Selected bond lengths (Å) and bond angles (°) of compounds **6–8**

	6	7	8
Bond lengths (Å)			
Cu1–P1	2.1387(9)	2.1750(10)	2.2092(8)
Cu2–P2	2.1459(9)	2.1662(11)	2.2208(8)
Cu1–X1	2.3591(8)	2.6003(6)	2.6526(4)
Cu2–X2	2.3716(8)	2.5246(6)	2.6560(4)
P1–N1	1.675(3)	1.687(3)	1.693(2)
P1–N2	1.670(3)	1.682(3)	1.696(2)
Bond angles (°)			
Cu1–P1–N1	123.74(10)	129.91(12)	122.68(9)
Cu1–P1–N2	125.99(10)	124.73(12)	125.25(10)
X1–Cu1–P1	131.18(3)	108.88(3)	122.32(3)
X2–Cu2–P2	125.12(3)	119.08(3)	118.23(2)

Table 3 Selected bond lengths (Å) and bond angles (°) of compound **15**

Bond lengths (Å)		Bond angles (°)	
Pd1–P1	2.244(3)	P1–Pd1–Cl1	100.40(10)
Pd1–Cl1	2.347(3)	C12–Pd1–P1	160.5(3)
Pd1–C12	2.213(10)	C12–Pd1–Cl1	98.6(3)
Pd1–C13	2.076(12)	C14–Pd1–P1	94.0(3)
Pd1–C14	2.118(11)	C14–Pd1–Cl1	165.3(3)
P1–N1	1.681(8)	N1–P1–Pd1	124.6(3)
P2–N2	1.665(8)	N1–P2–P1	42.5(3)
P1–O1	1.629(6)	N2–P2–N1	84.2(4)
P2–O2	1.626(6)	C1–O1–P1	125.3(6)

Phosphorus–phosphorus coupling constants

Phosphorus-31 chemical shifts and phosphorus–phosphorus coupling constants are very important parameters in understanding the structural features, reactivity and coordination properties of cyclodiphosphazane derivatives.

Phosphorus–phosphorus coupling constants are also related to the electron-supplying power of the phosphorus substituents and hence their coordinating abilities. The magnitude of coupling constants ($^2J_{PP}$) in cyclodiphosphazanes is highly dependent on the nature of the phosphorus substituents and the conformations adopted in solution under the influence of steric bulk of the phosphorus substituents. In view of this, it is very useful to compare the $^2J_{PP}$ coupling constants in various cyclodiphosphazane derivatives (Table 4) to get some insights into the conformations adopted by P–N bonds in solution and the coordinating abilities of phosphorus atoms. Generally, cyclodiphosphazanes of types **I–VII** show $^2J_{PP}$ couplings (Chart 2). The asymmetrically substituted cyclodiphosphazanes (**I**) generally show larger coupling constants (entries 1–6). Mixed chalcogen derivatives ($P_{(S/Se)}$–N–P_O) of types **II** and **III** (entries 7 and 14) show larger coupling constants compared to P_S–N–P_{Se} (entries 11 and 12) and $P_{(O/S/Se)}$–N–P derivatives (entries 8–10 and 13). The asymmetrically substituted cyclodiphosphazanes **II** and **III** also show larger coupling constants when one of the substituents on phosphorus is

Table 4 ^{31}P chemical shifts and $^{2}J_{PP}$ coupling constants in cyclodiphosphazane derivatives

Sl. no.	Compound	$^{a}\delta_P$	Structural type^{b}	$J_{PP}{}^{c}$ (Hz)	Ref.
	[{RP(E)(μ-N^{t}Bu)P(E)R′}$_2$]	—		—	—
1	R = Cl, R′ = F, E = lp	197 (PC1) & 180 (PF)	I	49.6	57
2	R = Cl, R′ = O^{t}Bu, E = lp	192 (PC1) (d) & 164 (d)	I	49.7	58
3	R = Cl, R′ = NH^{t}Bu, E = lp	201 (PC1) (d) & 136 (d)	I	45	6
4	R = Cl, R′ = OMe, E = lp	189 (PC1) (d) & 139 (d)	I	39.2	57
5	R = Cl, R′ = NMe$_2$, E = lp	187 (PCl) (d) & 131 (d)	I	32.5	57
6	R = Cl, R′ = Me, E = lp	237 (PCl) (d) & 200 (d)	I	33.0	57
7	R = (S)Cl, R′ = (O)Cl	36.0 (P_S) (d) & −4.3 (P_O)(d)	III	46	59
8	R = Cl, E = lp; R′ = Cl, E = O	132.4 (P) (d) & 6.2 (P_O) (d)	II	23	59
9	R = Cl E = O; R′ = Cl, E = S	147 (P_O) (d) & 61 (P_S) (d)	II	17	59
10	R = Cl, E = lp; R′ = Cl, E = Se	151 (P) (d) & 43 (P_{Se}) (d)	II	15	60
11	R = Cl, E = S; R′ = Cl, E = Se	43 (P_S) (d) & 21 (P_{Se}) (d)	III	6.5	60
12	R = H, E = S; R′ = NH^{t}Bu, E = Se	33 (P_S) (d) & 36 (P_{Se}) (d)	III	14	6
13	R = H, E = S; R′ = NH^{t}Bu, E = S;	37.2 (P_S) (d) & 104 (P_S) (d)	II	11.1	6
14	R = ^{t}BuNH, E = Se; R′ = H, E = O	20.9 (P_{Se}) (d) & −12.4 (P_O) (d)	III	22.7	61
15	R = ^{t}BuNH, R′ = (μ-OCH$_2$)$_2$, E = Se	24.4 (d) & 45.8 (d)	III	18.0	49
16	R = (^{t}BuNH), R′ = (μ-OCH$_2$)$_2$, E = S	37 (d) & 51 (d)	III	16.2	49
17	R = (*o*-OCH$_2$C$_5$H$_4$N), E = lp; R′ = (*o*-OCH$_2$C$_5$H$_4$N), E = Se	94 (P) (d) & 51 (P_{Se}) (d)	II	16.8	62
18	R = (*o*-OCH$_2$C$_5$H$_4$N), E = S; R′ = (*o*-OCH$_2$C$_5$H$_4$N), E = Se	49 (P_S) (d) & 41 (P_{Se}) (d)	III	15.0	62
19	R = (*o*-OCH$_2$C$_5$H$_4$N), E = lp; R′ = (*o*-OCH$_2$C$_5$H$_4$N), E = S	92 (P) (d) & 57 (P_S) (d)	II	14.0	62
[M{R((μ-N^{t}BuPE)$_2$)R′}]					
20	[{RuCl$_2$(η^6-*p*-cymene)}{R{(μ-N^{t}BuP)$_2$}R′}-*k*-P], R = ^{t}BuNH, R′ = H, E = O	P_c 62.7 (d) & P_u −6.4 (d)	IV	16.8	61
21	[{Cr(CO)$_4$}{(μ-N^{t}BuP(OPh))$_2$-*k*-P}$_2$]	P_c 182 (d) & P_u 128 (d)	V	10	63
22	[{RhCl(COD)}{(μN^{t}BuP(OPh))$_2$-*k*-P}]	P_c 107 (d) & P_u 129 (d)	IV	24.1	63
23	[{PtCl$_2$}{(μ-N^{t}BuP(OPh))$_2$-*k*-P}$_2$]	P_c 44.5 (dd) & P_u 126 (dd)	V	7.6	63
24	[{RuCl$_2$(η^6-*p*-cymene)}{(μ-N^{t}BuP(OC$_6$H$_4$OMe-*o*))$_2$-*k*-P}]	P_c 110 (d) & P_u 133 (d)	IV	8.7	23
25	[{PdCl$_2$}{(μ-N^{t}BuP(OC$_6$H$_4$OMe-*o*))$_2$-*k*-P}$_2$]	P_c 68 (d) & P_u 121 (d)	V	53	23
26	[{PtCl$_2$}{(μ-N^{t}BuP(OC$_6$H$_4$OMe-*o*))$_2$-*k*-P}$_2$]	P_c 40 (d) & P_u 126 (d)	V	7.3	23
[M{(RP(μ-N^{t}Bu)$_2$PR′)}M′]					
27	[RhCl(COD){(RP(μ-N^{t}Bu)$_2$PR′)}{AuCl}], R = R′ = OC$_6$H$_4$OMe-*o*	105 (P_{Au}) (dd) & 94 (P_{Rh}) (dd)	VI	30	64
28	[RhCl(COD){(RP(μ-N^{t}Bu)$_2$PR′)}{PdCl(η^3-C$_3$H$_5$)}], R = R′ = OC$_6$H$_4$OMe-*o*	131 (P_{Pd}) (d) & 94 (P_{Rh}) (dd)	VI	37	64
[M{RP(μ-N^{t}Bu)$_2$PR}M]					
29	[{(CO)Rh(μ-Cl)}$_4$}{RP(μ-N^{t}Bu)$_2$PR}$_2$], R = OCH$_2$CH$_2$OMe	117 (m)	VII	42	23
30	[{Rh(CO)Cl}$_2$}{RP(μ-N^{t}Bu)$_2$PR}-*k*-P, *k*-N], R = OCH$_2$CH$_2$NMe$_2$	124 (m)	VII	44	23
31	[{Rh(CO)Cl}$_2$}{RP(μ-N^{t}Bu)$_2$PR}-*k*-P, *k*-S]; R = OCH$_2$CH$_2$SMe	122 (m)	VII	45	23
32	[{RuCl$_2$(η^6-*p*-cymene)}$_2$}{(μ-N^{t}BuP(C≡CPh))$_2$}-*k*-P]	127 (d) & 129 (d)	VII	11	65
33	[{RhCl(COD)}$_2$}{Fe(η^5-C$_5$H$_4$)$_2$(μ-N^{t}BuP)$_2$}-*k*-P]	149	VII	^{d}	56
34	[{(CO)Rh(μ-Cl)}$_2$}{RP(μ-N^{t}Bu)$_2$PR}]$_2$; R = OC$_6$H$_4$OMe-*o*	116 (m)	VII	47	22
35	[{RuCl$_2$(η^6-*p*-cymene)}$_2$}{(μ-N(^{t}Bu)P)$_2$(C$_6$H$_4$O$_2$)}]	140 (d) & 128 (d)	VII	45.4	This work
36	[{(μN(^{t}Bu)P)$_2$(C$_6$H$_4$O$_2$)(RhCl-(COD))}$_2$]	125 (dd) & 124 (dd)	VII	27.2	This work
37	[{RuCl$_2$(η^6-*p*-cymene)}$_4$}{((μ-N(^{t}Bu)P)$_2$)$_2$(μ-C$_6$H$_2$O$_4$)}]	142 (d) & 130 (d)	VII	44.5	This work
38	[{RhCl(COD)}$_4$}{((μ-N(^{t}Bu)P)$_2$)$_2$(μ-C$_6$H$_2$O$_4$)}]	125 (dd) & 125 (dd)	VII	26.8	This work

^{a} δ in ppm. ^{b} Chart 2. ^{c} In all these compounds, phosphorus atoms are two bonds apart and J_{MP} coupling is ignored. ^{d} ($^{2}J_{PP}$) coupling was not observed. P_u, uncoordinated phosphorus, P_c, coordinated phosphorus. lp = lone pair.

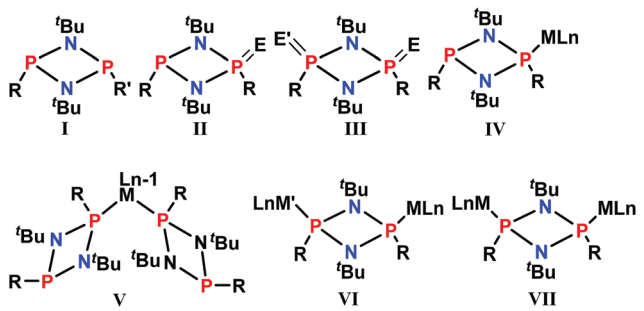

Chart 2 Cyclodiphosphazanes with non-equivalent phosphorus atoms with $^{2}J_{PP}$ couplings.

relatively more electronegative. However, significantly different coupling constants are observed for cyclodiphosphazanes **IV–VII**. Again, in the conformational isomers of type **VII**, $^{2}J_{PP}$ coupling is dictated by the oxidation state of the metal centers and the orientation of the phosphorus substituents. If the phosphorus substituents are conformationally same, a single resonance is observed in the $^{31}P\{^{1}H\}$ NMR, as in the case of [{RhCl(COD)}$_2$}{Fe(η^5-C$_5$H$_4$)$_2$(μ-N^{t}BuP)$_2$}-*k*-P][56] (entry 33), and hence no $^{2}J_{PP}$ coupling. Ruthenium and rhodium complexes of **1** and **2** showed $^{2}J_{PP}$ couplings due to the phosphorus substituents having different conformations, which was also confirmed by their solid state X-ray analysis. As evident from Table 4, the ruthenium(II) complexes of **1** and **2** (entries 35 and 37) showed larger coupling constants compared to the rhodium(I) complexes (entries 36 and 38). This may be due to the electropositive nature of the ruthenium metal.

Table 5 Crystallographic information of compounds **2–6**

	2	**3**	**4**	**5**	**6**
Empirical formula	$C_{22}H_{38}N_4O_4P_4$	$C_{18}H_{28}Cl_2Cu_2N_4O_2P_2$	$C_{32}H_{50}Br_2Cu_2N_6O_4P_4$	$C_{32}H_{50}Cu_2I_2N_6O_4P_4$	$C_{28}H_{44}Cl_4Cu_4N_4O_6P_4$
Formula weight	546.44	592.36	993.56	1087.54	1020.51
Space group	Trigonal	Triclinic	Triclinic	Triclinic	Monoclinic
Crystal system	$R\bar{3}$	$P\bar{1}$	$P\bar{1}$	$P\bar{1}$	$P2_1/c$
a/Å	34.968(2)	8.5545(3)	9.22027(18)	9.2630(3)	14.9560(6)
b/Å	34.968(2)	8.8157(3)	12.2451(2)	12.1825(3)	16.3767(7)
c/Å	6.2485(3)	17.6978(5)	18.8242(3)	18.6917(7)	17.6289(7)
α/°	90	87.933(3)	86.8260(14)	88.319(2)	90
β/°	90	87.232(3)	79.3340(16)	82.651(3)	101.459(4)
γ/°	120	63.913(4)	84.3383(15)	84.948(2)	90
Volume/Å^3	6616.7(9)	1197.13(8)	2076.91(7)	2083.49(12)	4231.8(3)
Z	9	2	2	2	4
ρ_{calc}, (g cm^{-3})	1.234	1.643	1.589	1.734	1.602
μ (Mo Kα), mm^{-1}	0.289	2.156	3.144	2.698	2.423
F(000)	2610.0	604.0	1008.0	1080.0	2064.0
Size	0.27 × 0.04 × 0.03	0.14 × 0.09 × 0.06	0.21 × 0.16 × 0.06	0.22 × 0.07 × 0.03	0.14 × 0.09 × 0.04
T (K)	150	150	150	150	150
2θ range, °	4.66–49.99	4.61–49.994	3.93–50	3.35–49.992	4.69–49.994
Reflections collected	7348	13 336	40 973	32 062	49 799
Independent reflections	2574[R_{int} = 0.0715]	4051 [R_{int} = 0.0236]	7296 [R_{int} = 0.0658]	7309 [R_{int} = 0.0550]	7434 [R_{int} = 0.0764]
S	1.039	1.047	1.035	1.040	1.038
R_1	0.0483	0.0244	0.0347	0.0319	0.0352
wR_2	0.1201	0.0640	0.0875	0.0715	0.0886

Table 6 Crystallographic information of compounds **7**, **8** and **15**

	7	**8**	**15**
Formula	$C_{28}H_{44}Br_4Cu_4N_4O_4P_4$	$C_{28}H_{44}Cu_4I_4N_4O_4P_4$	$C_{34}H_{58}Cl_4N_4O_4P_4Pd_4$
Formula Weight	1198.35	1386.31	1278.12
Crystal System	Monoclinic	Monoclinic	Monoclinic
Space group	$P2_1/n$	$P2_1/n$	$P2_1/c$
a, Å	15.3981(9)	15.4007(6)	16.4158(13)
b, Å	16.3342(10)	16.7327(5)	10.4693(7)
c, Å	17.8607(11)	18.1852(7)	17.2657(16)
α, °	90	90	90
β, °	113.0690(10)	113.290(4)	110.152(10)
γ, °	90	90	90
V, Å^3	4133.0(4)	4304.4(3)	2785.7(4)
Z	4	4	2
ρ_{calc}, (g cm^{-3})	1.926	2.139	1.524
μ (Mo Kα), mm^{-1}	6.089	5.003	1.610
F (000)	2352.0	2640	1268.0
Crystal size, mm	0.24 × 0.18 × 0.14	0.16 × 0.15 × 0.04	0.23 × 0.08 × 0.06
T (K)	100	150	150
2θ range, °	3.51–49.99	5.07–50	4.70–49.99
Total no. of reflections	58 368	27 214	20 568
No. of independent reflections	7277 [R_{int} = 0.0489]	7575 [R_{int} = 0.0274]	4889[R_{int} = 0.1129]
S	1.021	1.100	1.040
R_1	0.0294	0.0202	0.0722
wR_2	0.0782	0.0461	0.1900

The distortion from pyramidal geometry at phosphorus atoms increases the s-character of the lone pair of the phosphorus center due to which ^{31}P NMR chemical shifts go downfield in these cases; more distortion in the geometry probably causes diamagnetic deshielding effect (magnetic anisotropy) and in turn influences the magnitude of the $^2J_{PP}$ coupling constant. However, in order to determine the nature of $^2J_{PP}$ coupling in metal complexes, the contributions coming from both the pathways, (i) *via* ligand framework (P–N–P) and (ii) through metal (P–M–P), have to be considered and warrant further investigation.

Conclusions

Synthesis of two new catechol and 1,2,4,5-tetrahydroxybenzene functionalized cyclodiphosphazanes and their coordination complexes with Cu^{I}, Ru^{II}, Rh^{I}, Pd^{II} and Au^{I} are described. Both the cyclodiphosphazanes show interesting coordination properties. The reaction of the catechol derivative with CuX (X = Cl, Br, I) in varying stoichiometries afforded 1-D and 2-D coordination polymers, depending upon the reaction conditions used. In 1-D coordination polymer **3**, the propagation

of the polymeric chain is through the formation of rhombic $[Cu(\mu\text{-}Cl)]_2$ units, whereas in **4** and **5**, cyclodiphosphazane links discrete CuX(S) fragments (X = halide, S = CH_3CN) on either side to form 1-D coordination polymers. In the case of 2-D coordination polymers (**6–8**), the propagation of the polymeric chain involves $[Cu_4(\mu_3\text{-}X)_4]$ cuboids. Cyclodiphosphazanes **1** or **2** on treatment with various platinum metal precursors afforded corresponding di- or tetranuclear complexes, with the cyclodiphosphazanes exhibiting a bridging mode of coordination. Further utility of these complexes in catalytic reactions and host–guest chemistry is under active investigation in our laboratory.

Experimental section

General procedures

Unless specified otherwise, all manipulations were carried out using the standard Schlenk line and glovebox techniques under an atmosphere of dry nitrogen or argon. All the solvents were dried by conventional methods and distilled prior to use. The compounds *cis*-$[ClP(\mu\text{-}N^tBu)]_2$,[26] CuCl,[66] CuBr,[66] $[RuCl_2(\eta^6\text{-cymene})]_2$,[67] $[Pd(\eta^3\text{-}C_3H_5)Cl]_2$,[68] $[AuCl(SMe_2)]$[69] and $[Rh(COD)Cl]_2$[70] were prepared according to the published procedures. CuI was purchased from Aldrich chemicals and used as such without further purification. Other chemicals were obtained from commercial sources and purified prior to use.

Instrumentation

NMR spectra were recorded on Bruker FT spectrometers (Avance-400 or 500 MHz) at ambient probe temperatures. $^{13}C\{^1H\}$ and $^{31}P\{^1H\}$ NMR spectra were acquired using the broad band decoupling method. The spectra were recorded in $CDCl_3$ solutions with TMS as an internal standard; the chemical shifts of ^1H and $^{13}C\{^1H\}$ NMR spectra are reported in ppm downfield from TMS. The chemical shifts of $^{31}P\{^1H\}$ NMR spectra are referred to 85% H_3PO_4 as an external standard. Positive values indicate downfield shifts. Mass spectra were recorded using a Bruker Maxis Impact LC-q-TOF Mass Spectrometer. Infrared spectra were recorded on a PerkinElmer *Spectrum One* FT-IR Spectrometer (Model No. 73465) in KBr disk. The microanalyses were performed using a Thermo Finnigan FLASH EA 1112 Series CHNS Analyzer. The melting points of all compounds were determined on a Veego melting point apparatus and are uncorrected.

Synthesis of $[\{(\mu\text{-}N(^tBu)P)_2(C_6H_4O_2)\}]$ (1)

To a stirred solution of catechol (1.040 g, 9.445 mmol) and Et_3N (3.84 mL, excess) in diethyl ether (20 mL) was added dropwise a solution of *cis*-$[ClP(\mu\text{-}N^tBu)]_2$ (2.598 g, 9.445 mmol) also in diethyl ether (20 mL) at 0 °C. The reaction mixture was allowed to warm to the room temperature and stirred further for a period of 16 h. Then it was filtered and dried under vacuum to give **1** as white oily liquid which was redissolved in 20 mL of diethyl ether, passed through a pad of activated silica gel, concentrated to a small bulk (3 mL) and stored for 24 h to afford the analytically pure product of **1** as white solid. Yield 85% (2.508 g). Mp: 73–76 °C. Anal. calcd for $C_{14}H_{22}O_2P_2N_2$: C, 53.85; H, 7.10; N, 8.97. Found: C, 53.73; H, 8.54; N 8.61. ^1H NMR (400 MHz, $CDCl_3$) δ 7.32–7.27 (m, 2H, ArH), 7.05–7.00 (m, 2H, ArH), 1.10 (s, 18H, ^{t}Bu). $^{13}C\{^1H\}$ NMR (101 MHz, $CDCl_3$) δ 146.26 (t, J = 4.9 Hz), 124.35 (s), 122.98 (s), 51.43 (t, J = 7.1 Hz), 30.41 (t, J = 5.7 Hz). $^{31}P\{^1H\}$ NMR (162 MHz, $CDCl_3$) δ 180.9 (s). FT-IR (KBr disk, cm^{-1}): 2967 s, 2929 w, 2867 w, 1651 m, 1489 s, 1478 s, 1394 m, 1365 s, 1293 s, 1260 m, 1212 s, 1092 m, 1046 s, 931 m, 918 w, 862 w, 768 w, 714 w. ESI-MS: m/z calcd for $C_{14}H_{23}O_2P_2N_2$ $(M + H)^+$ 313.1260, found 313.1229.

Synthesis of $[\{((\mu\text{-}N(^tBu)P)_2)_2(\mu\text{-}C_6H_2O_4)\}]$ (2)

To a solution of tetrahydroxybenzene (0.503 g, 3.539 mmol) and Et_3N (3.0 mL, excess) in THF (40 mL) was added dropwise a solution of *cis*-$[ClP(\mu\text{-}N^tBu)]_2$ (1.947 g, 7.077 mmol) also in THF (30 mL) at 0 °C, and the reaction mixture was warmed to room temperature and stirred further for a period of 16 h. The solution was passed through a pad of activated silica gel and the solvent was evaporated under reduced pressure to afford the analytically pure product of **2** as microcrystalline solid. Crystals suitable for X-ray structure analysis were obtained by slow diffusion of a dichloromethane solution of **2** layered with hexane at room temperature. Yield 87% (1.690 g). Mp: 198–203 °C. Anal. calcd for $C_{22}H_{38}N_4O_4P_4$: C, 48.35; H, 7.01; N, 10.25. Found: C, 48.25; H, 7.00; N 10.30. ^1H NMR (500 MHz, $CDCl_3$) δ 7.17 (s, 2H, ArH), 1.11 (s, 36H, ^{t}Bu). $^{13}C\{^1H\}$ NMR (126 MHz, $CDCl_3$) δ 141.42 (t, J = 4.8 Hz), 117.49 (s), 51.41 (s), 30.41 (t, J = 5.6 Hz). $^{31}P\{^1H\}$ NMR (202 MHz, $CDCl_3$) δ 181.6 (s). FT-IR (KBr disk, cm^{-1}): 2972 s, 2864 w, 1481 s, 1395 w, 1366 s, 1269 w, 1213 s, 1161 s, 1051 s, 939 s, 902 s, 804 s. ESI-MS: m/z calcd for $C_{22}H_{39}N_4O_4P_4$ $(M + H)^+$ 547.1916, found 547.1913.

Synthesis of $[\{(\mu\text{-}N(^tBu)P)_2(C_6H_4O_2)\}\{Cu(\mu_2\text{-}Cl)(NCCH_3)\}_2]_n$ (3)

A solution of CuCl (0.006 g, 0.064 mmol) in acetonitrile (7 mL) was added dropwise to a well stirred solution of **1** (0.020 g, 0.064 mmol) also in dichloromethane (5 mL), and the reaction mixture was stirred for 6 h at room temperature. The solvent was evaporated under vacuum to give **3** as a colourless residue which was washed with petroleum ether (1 × 10 mL) to get the analytically pure product of **3** as colorless microcrystalline solid. Yield: 47% (0.009 g). Mp: 210–216 °C (dec.). Anal. calcd for $C_{18}H_{28}O_2P_2N_4Cu_2Cl_2$: C, 36.50; H, 4.76; N, 9.46. Found: C, 36.48; H, 4.90; N 9.14. FT-IR (KBr disk, cm^{-1}): 3068 m, 2969 s, 2904 m, 2830 w, 2742 w, 2634 m, 2541 w, 2417 m (ν_{CN}), 2398 m (ν_{CN}), 1632 w, 1546 w, 1478 s, 1397 m, 1367 s, 1294 s, 1249 m, 1208 s, 1136 m, 1090 s, 1055 s, 934 m, 888 s, 757 s, 606 m.

Synthesis of $[\{(\mu\text{-}N(^tBu)P)_2(C_6H_4O_2)\}\{CuBr(NCCH_3)\}]_n$ (4)

A solution of CuBr (0.010 g, 0.069 mmol) in acetonitrile (7 mL) was added dropwise to a well stirred solution of **1** (0.022 g, 0.069 mmol) in the same solvent (5 mL), and the reaction mixture was stirred for 6 h at room temperature. The solvent was evaporated under vacuum and the residue thus obtained was washed with petroleum ether (2 × 8 mL) and filtered to

give the analytically pure product of **4** as white crystalline solid. Yield: 75% (0.026 g). Mp: 195–198 °C (dec.). Anal. calcd for $C_{32}H_{50}O_4P_4N_6Cu_2Br_2$: C, 38.68; H, 5.07; N, 8.46. Found: C, 38.85; H, 5.28; N 8.57. FT-IR (KBr disk, cm^{-1}): 2969 s, 2905 m, 2835 w, 2744 w, 2637 w, 2542 w, 2398 m (ν_{CN}), 1632 w, 1546 w, 1478 s, 1367 s, 1293 s, 1202 s, 1147 m, 1089 s, 1055 s, 915 s, 875 s, 757 s, 604 m.

Synthesis of $[\{(\mu\text{-}N(^tBu)P)_2(C_6H_4O_2)\}\{CuI(NCCH_3)\}]_n$ (5)

A solution of CuI (0.009 g, 0.047 mmol) in acetonitrile (7 mL) was added dropwise to a well stirred solution of **1** (0.015 g, 0.047 mmol) also in (5 mL) dichloromethane. The reaction mixture was stirred for 6 h at room temperature followed by evaporation of solvents under vacuum to afford **5** as colourless solid; the residue thus obtained was washed with petroleum ether (1 × 8 mL) to get the analytically pure product **5** as microcrystalline solid. Yield: 74% (0.019 g). Mp: 178–183 °C (dec.). Anal. calcd for $C_{32}H_{50}N_6O_4P_4Cu_2I_2$: C, 35.34; H, 4.63; N, 7.73. Found: C, 34.89; H, 4.84; N, 7.64. FT-IR (KBr disk, cm^{-1}): 2969 s, 2905 m, 2835 w, 2744 w, 2635 w, 2541 w, 2397 m (ν_{CN}), 1632 w, 1478 s, 1394 m, 1367 s, 1352 w, 1208 s, 1146 m, 1089 s, 1055 s, 915 s, 757 s, 604 m.

Synthesis of $[\{(\mu\text{-}N(^tBu)P)_2(C_6H_4O_2)\}_2\{Cu_4(\mu_3\text{-}Cl)_4\}]_n$ (6)

A solution of CuCl (0.013 g, 0.131 mmol) in acetonitrile (10 mL) was added dropwise to a solution of **1** (0.020 g, 0.065 mmol) in dichloromethane (10 mL) and stirred for 4 h at room temperature. The solvent was evaporated under reduced pressure and the residue obtained was washed with petroleum ether (2 × 6 mL) and the solution was filtered to get analytically pure product of **6** as crystalline solid. Yield: 84% (0.028 g). Mp: 248–254 °C (dec.). Anal. calcd for $C_{28}H_{44}N_4O_4P_4Cu_4Cl_4$: C, 32.95; H, 4.35; N, 5.49. Found: C, 32.52; H, 4.64; N, 5.67. ^{1}H NMR (500 MHz, DMSO-d_6) δ 7.30 (dd, J = 6.0, 3.7 Hz, 2H, ArH), 7.18 (dd, J = 6.2, 3.6 Hz, 2H, ArH), 1.19 (s, 18H, ^{t}Bu). ^{31}P $\{^1$H$\}$ NMR (161.9 MHz, DMSO-d_6): δ 122.5 (s). FT-IR (KBr disk, cm^{-1}): 3066 m, 2969 s, 2903 w, 2868 w, 2637 m, 1566 w, 1546 w, 1547 w, 1478 s, 1396 m, 1368 s, 1294 s, 1249 m, 1202 s, 1169 m, 1090 s, 1054 s, 917 s, 890 s, 806 m, 758 s, 606 m.

Synthesis of $[\{(\mu\text{-}N(^tBu)P)_2(C_6H_4O_2)\}_2\{Cu_4(\mu_3\text{-}Br)_4\}]_n$ (7)

A solution of CuBr (0.014 g, 0.097 mmol) in acetonitrile (10 mL) was added dropwise to a well stirred solution of **1** (0.015 g, 0.049 mmol) in dichloromethane (10 mL). The workup procedure was similar to that described for **6**, which resulted in the pure product of **7** as colorless crystalline solid. Yield: 82% (0.024 g). Mp: 219–225 °C (dec.). Anal. calcd for $C_{28}H_{44}N_4O_4P_4Cu_4Br_4$: C, 28.06; H, 3.70; N, 4.68. Found: C, 28.40; H, 3.66; N, 4.89. ^{1}H NMR (500 MHz, DMSO-d_6) δ 7.34–7.29 (m, 2H, ArH), 7.23–7.18 (m, 2H, ArH), 1.22 (s, 18H, ^{t}Bu). ^{31}P$\{^1$H$\}$ NMR (161.9 MHz, DMSO-d_6): δ 120.3 (s). FT-IR (KBr disk, cm^{-1}): 3074 w, 2969 s, 2864 m, 2633 w, 1571 m, 1478 s, 1438 m, 1396 w, 1368 s, 1297 s, 1206 s, 1169 m, 1090 s, 1068 s, 917 s, 889 s, 871 m, 757 s, 606 m.

Synthesis of $[\{(\mu\text{-}N(^tBu)P)_2(C_6H_4O_2)\}_2\{Cu_4(\mu_3\text{-}I)_4\}]_n$ (8)

A solution of CuI (0.014 g, 0.075 mmol) in acetonitrile (10 mL) was added dropwise to a well stirred solution of **1** (0.012 g, 0.037 mmol) in dichloromethane (10 mL). The workup procedure was similar to that described for **6**, which resulted in the analytically pure product **8** as colorless crystalline solid. Yield: 84% (0.022 g). Mp: 208–211 °C (dec.). Anal. calcd for $C_{28}H_{44}N_4P_4O_4Cu_4I_4$: C, 24.26; H, 3.20; N, 4.04. Found: C, 24.09; H, 3.53; N, 4.30. ^{1}H NMR (500 MHz, DMSO-d_6) δ 7.31 (dd, J = 5.9, 3.7 Hz, 2H, ArH), 7.19 (dd, J = 6.0, 3.7 Hz, 2H, ArH), 1.23 (s, 18H, ^{t}Bu). ^{31}P$\{^1$H$\}$ NMR (161.9 MHz, DMSO-d_6): δ 125.2 (s). FT-IR (KBr disk, cm^{-1}): 3071 w, 2967 s, 2542 w, 1568 w, 1478 s, 1438 m, 1396 w, 1368 s, 1297 s, 1206 s, 1169 m, 1090 s, 1068 s, 917 s, 889 s, 871 m, 757 s, 606 m.

Synthesis of $[\{(\mu\text{-}N(^tBu)P)_2(C_6H_4O_2)\}\{RuCl_2(\eta^6\text{-}p\text{-cymene})\}_2]$ (9)

A solution of $[RuCl_2(\eta^6\text{-}p\text{-cymene})]_2$ (0.021 g, 0.034 mmol) in dichloromethane (7 mL) was added dropwise to a solution of **1** (0.010 g, 0.034 mmol) also in dichloromethane (7 mL). The reaction mixture was stirred at room temperature for 4 h. After the complete removal of the solvent under reduced pressure, the residue thus obtained was washed with petroleum ether to the give analytically pure product of **9** as red solid. Yield: 89% (0.028 g). Mp: 198–202 °C(dec.). Anal. calcd for $C_{34}H_{50}N_2P_2O_2Ru_2Cl_4$: C, 44.16; H, 5.45; N, 3.03. Found: C, 44.43; H, 5.62; N, 3.29. ^{1}H NMR (400 MHz, $CDCl_3$) δ 7.33 (dd, J = 8.1, 5.4 Hz, 2H, ArH), 7.15 (dd, J = 6.8, 3.2 Hz, 2H, ArH), 5.69–5.60 (m, 6H, p-cymene), 5.39 (d, J = 5.6 Hz, 2H, p-cymene), 3.27–3.16 (m, 1H, $(CH_3)_2CH$), 3.08 (m, 1H, $(CH_3)_2CH$), 2.43 (s, 3H, $ArCH_3$), 2.34 (s, 3H, $ArCH_3$), 1.42 (s, 18H, ^{t}Bu), 1.36 (d, J = 6.9 Hz, 12H, $(CH_3)_2CH$). ^{31}P$\{^1$H$\}$ NMR (202 MHz, $CDCl_3$) δ 140.4 (d, J = 45.1 Hz), 127.9 (d, J = 45.4 Hz). FT-IR (KBr disk, cm^{-1}): 2969 s, 2871 m, 1633 m, 1480 s, 1438 m, 1396 w, 1363 m, 1298 s, 1260 s, 1215 m, 892 s, 859 m, 816 w, 769 w, 589 m. ESI-MS: m/z calcd for $C_{34}H_{50}Cl_3N_2O_2P_2Ru_2$ $(M - C1)^+$: 891.0499, found: 891.0460.

Synthesis of $[\{(\mu\text{-}N(^tBu)P)_2(C_6H_4O_2)\}\{RhCl(COD)\}_2]$ (10)

A solution of $[Rh(COD)Cl]_2$ (0.020 g, 0.040 mmol) in dichloromethane (7 mL) was added dropwise to a solution of **1** (0.013 g, 0.040 mmol) in the same solvent (8 mL), and the solution was stirred at room temperature for 4 h. The solution was concentrated to a small bulk under reduced pressure and stored at 0 °C for 24 h to give **10** as yellow crystalline solid. Yield: 81% (0.026 g). Mp: 235–238 °C (dec.). Anal. calcd for $C_{30}H_{46}O_2P_2N_2Rh_2Cl_2$: C, 44.74; H, 5.76; N, 3.48. Found: C, 44.53; H, 5.98; N, 3.25. ^{1}H NMR (500 MHz, $CDCl_3$) δ 7.43 (d, J = 7.6 Hz, 1H, ArH), 7.08 (d, J = 7.6 Hz, 1H, ArH), 7.06–7.01 (m, 1H, ArH), 6.94 (d, J = 7.7 Hz, 1H, ArH), 5.80 (d, J = 42.7 Hz, 4H, CH), 4.54 (s, 1H, CH), 4.23 (s, 1H, CH), 4.00 (s, 2H, CH), 2.42 (dd, J = 34.0, 26.5 Hz, 8H, CH_2), 2.24 (d, J = 20.5 Hz, 8H, CH_2), 1.52 (s, 18H, ^{t}Bu). ^{31}P$\{^1$H$\}$ NMR (202 MHz, $CDCl_3$) δ 124.7 (dd, $^1J_{RhP}$ = 246.9 Hz, $^2J_{PP}$ = 27.2 Hz), 124.2 (dd, $^1J_{RhP}$ = 240.9, $^2J_{PP}$ = 27.2 Hz). FT-IR (KBr disk, cm^{-1}): 2970 m, 2883 m, 1651 s, 1480 m, 1367 m, 1299 s, 1214 m, 1093 m, 1045 m, 915 m,

894 m, 859 m, 755 w, 606 m. ESI-MS: *m*/*z* calcd for $C_{30}H_{46}ClO_2P_2N_2Rh_2$ $(M - Cl)^+$ 769.0828, found 769.0791.

Synthesis of [{(μ-N(ᵗBu)P)$_2$(C$_6$H$_4$O$_2$)}{PdCl(η^3-C$_3$H$_5$)}$_2$] (11)

A solution of $[Pd(\eta^3\text{-}C_3H_5)Cl]_2$ (0.016 g, 0.043 mmol) in dichloromethane (5 mL) was added dropwise to a well stirred solution of **1** (0.013 g, 0.043 mmol) also in dichloromethane (5 mL), and stirring was continued for 6 h. The solution was concentrated to a small bulk and stored at 10 °C for 24 h to give the analytically pure product of **11** as yellow microcrystalline solid. Yield: 82% (0.024 g). Mp: 238–241 °C (dec.). Anal. calcd for $C_{20}H_{32}O_2P_2N_2Pd_2Cl_2$: C, 35.42; H, 4.76; N, 4.13. Found: C, 35.69; H, 4.52; N, 4.29. ^{1}H NMR (400 MHz, $CDCl_3$) δ 7. 38 (dd, J = 6.2, 3.7 Hz, 2H, ArH), 7.16 (dd, J = 6.2, 3.7 Hz, 2H, ArH), 5.69 (dt, J = 20.1, 10.0 Hz, 2H, η^3-C_3H_5), 4.84 (s, 2H, η^3-C_3H_5), 4.58 (s, 2H, η^3-C_3H_5), 3.78 (s, 1H, η^3-C_3H_5), 3.13 (s, 2H, η^3-C_3H_5), 1.29 (s, 18H, ᵗBu). $^{31}P\{^1H\}$ NMR (202 MHz, $CDCl_3$): 135.2 ppm. FT-IR (KBr disk, cm^{-1}): 2976 m, 1645 s, 1482 m, 1385 w, 1367 m, 1272 w, 1192 w, 1161 m, 1069 m, 947 m, 900 m. ESI-MS: *m*/*z* calcd for $C_{20}H_{32}Cl_2KN_2O_2P_2Pd_2$ $(M + K)^+$ 716.9019, found 716.8933.

Synthesis of [{(μ-N(ᵗBu)P)$_2$(C$_6$H$_4$O$_2$)}{AuCl}$_2$] (12)

A solution of $AuCl(SMe_2)$ (0.016 g, 0.054 mmol) in dichloromethane (9 mL) was added dropwise to a solution of **1** (0.009 g, 0.027 mmol) in the same solvent (6 mL), and the reaction mixture was stirred at room temperature for 4 h. The solution was concentrated to a small bulk and stored at room temperature for 24 h to give **12** as white crystalline solid. Yield: 80% (0.018 g). Mp: 153–157 °C (dec.). Anal. calcd for $C_{14}H_{22}O_2P_2N_2Au_2Cl_2$: C, 21.63; H, 2.85; N, 3.60. Found: C, 21.25; H, 2.97; N 3.38. ^{1}H NMR (500 MHz, $CDCl_3$) δ 7.38 (dt, J = 7.0, 3.5 Hz, 2H, ArH), 7.35–7.31 (m, 2H, ArH), 1.41 (s, 18H, ᵗBu). $^{31}P\{^1H\}$ NMR (202 MHz, $CDCl_3$): δ 117.4 (s). ESI-MS: *m*/*z* calcd for $C_{14}H_{22}AgAu_2Cl_2N_2O_2P_2$ $(M + Ag)^+$ 884.8897, found 884.5098.

Synthesis of [{((μ-N(ᵗBu)P)$_2$)$_2$(μ-C$_6$H$_2$O$_4$)}{RuCl$_2$(η^6-*p*-cymene)}$_4$] (13)

A solution of $[RuCl_2(\eta^6\text{-}p\text{-cymene})]_2$ (0.069 g, 0.112 mmol) in dichloromethane (7 mL) was added dropwise to a solution of **2** (0.031 g, 0.056 mmol) also in dichloromethane (7 mL), and the reaction mixture was stirred at room temperature for 4 h. After the complete removal of the solvent under reduced pressure, the red color residue obtained was washed with petroleum ether, redissolved in 3 mL of dichloromethane and stored at 10 °C for 24 h to give crystalline solid of **13**. Yield: 70% (0.070 g). Mp: 208–210 °C (dec.). Anal. calcd for $C_{62}H_{94}Cl_8N_4O_4P_4Ru_4$: C, 42.04; H, 5.35; N, 3.16. Found: C, 42.11; H, 5.38; N, 3.00. ^{1}H NMR (500 MHz, $CDCl_3$) δ 7.29 (s, 2H, ArH), 5.74–5.65 (m, 12H, *p*-cymene), 5.40 (d, J = 5.7 Hz, 4H, *p*-cymene), 3.25–3.16 (m, 2H, $(CH_3)_2CH$), 2.87–2.77 (m, 2H, $(CH_3)_2CH$), 2.43 (s, 6H, $ArCH_3$), 2.19 (s, 6H, $ArCH_3$), 1.44 (s, 36H, ᵗBu), 1.39 (d, J = 5.9 Hz, 24H, $(CH_3)_2CH$).$^{31}P\{^1H\}$ NMR (202 MHz, $CDCl_3$) δ 142.3 (d, J = 44.3 Hz), 129.65 (d, J = 44.5 Hz). FT-IR (KBr disk, cm^{-1}): 2976 m, 2925 m, 1644 s, 1520 w, 1482 w, 1263 m, 1216 m, 1163 m, 1051 w, 1018 w, 944 s, 888 m, 667 m, 635 m. ESI-MS: *m*/*z* calcd for $C_{62}H_{94}Cl_7N_4O_4P_4Ru_4$ $(M - C1)^+$: 1736.0220, found: 1736.0452.

Synthesis of [{((μ-N(ᵗBu)P)$_2$)$_2$(μ-C$_6$H$_2$O$_4$)}{RhCl(COD)}$_4$] (14)

To a stirred solution of $[Rh(COD)Cl]_2$ (0.020 g, 0.040 mmol) in dichloromethane (7 mL) was added dropwise a solution of **2** (0.011 g, 0.020 mmol) also in dichloromethane (8 mL), and stirring was continued for a further period of 4 h. The solution was concentrated to a small bulk and stored at 0 °C for 24 h to give the analytically pure product of **14** as yellow solid. Yield: 77% (0.024 g). Mp: 235–238 °C (dec.). Anal. calcd for $C_{54}H_{86}Cl_4N_4O_4P_4Rh_4$: C, 42.32; H, 5.66; N, 3.66. Found: C, 42.27; H, 5.45; N, 3.46. ^{1}H NMR (500 MHz, $CDCl_3$) δ 7.00 (s, 2H, ArH), 5.79 (d, J = 31.8 Hz, 8H, CH), 4.52 (s, 4H, CH), 4.23 (s, 2H), 3.99 (s, 4H, CH), 2.52–2.35 (m, 20H, CH_2), 2.24 (d, J = 16.8 Hz, 16H, CH_2), 1.50 (s, 36H, ᵗBu). $^{31}P\{^1H\}$ NMR (202 MHz, $CDCl_3$) δ 125.5 (dd, $^1J_{RhP}$ = 246.9 Hz, $^2J_{PP}$ = 26.8 Hz), 124.9 (dd, $^1J_{RhP}$ = 242.8, $^2J_{PP}$ = 26.8 Hz). FT-IR (KBr disk, cm^{-1}): 2972 m, 2881 w, 2832 w, 1628 m, 1484 m, 1385 w, 1367 w, 1273 w, 1161 m, 1086 m, 944 m, 896 m. ESI-MS: *m*/*z* calcd for $C_{54}H_{86}Cl_3N_4O_4P_4Rh_4$ $(M - C1)^+$: 1497.0866, found: 1497.0907.

Synthesis of [{((μ-N(ᵗBu)P)$_2$)$_2$(μ-C$_6$H$_2$O$_4$)}{PdCl(η^3-C$_3$H$_5$)}$_4$] (15)

To a stirred solution of $[Pd(\eta^3\text{-}C_3H_5)Cl]_2$ (0.020 g, 0.054 mmol) in dichloromethane (7 mL) was added dropwise a solution of **2** (0.015 g, 0.027 mmol) also in dichloromethane (8 mL), and stirring was continued for 6 h. The solution was concentrated to 3 mL and 1 mL of hexane was added and cooled to 0 °C for 24 h to give **15** as pale green crystalline solid. Yield: 74% (0.026 g). Mp: 251–253 °C (dec.). Anal. calcd for $C_{34}H_{58}Cl_4N_4O_4P_4Pd_4$: C, 31.95; H, 4.57; N, 4.38. Found: C, 31.57; H, 4.28; N, 4.68. ^{1}H NMR (500 MHz, $CDCl_3$) δ 7.49 (s, 2H, ArH), 5.73 (t, J = 9.3 Hz, 4H, η^3-C_3H_5), 4.89 (s, 4H, η^3-C_3H_5), 4.68 (s, 4H, η^3-C_3H_5), 3.82 (t, J = 13.9 Hz, 4H, η^3-C_3H_5), 3.16 (d, J = 10.3 Hz, 4H, η^3-C_3H_5), 1.32 (s, 36H, ᵗBu). $^{31}P\{^1H\}$ NMR (202 MHz, $CDCl_3$): δ 137.4 (s) FT-IR (KBr disk, cm^{-1}): 2976 m, 1645 s, 1482 m, 1385 w, 1367 m, 1272 w, 1192 w, 1161 m, 1069 m, 947 m, 900 m. ESI-MS: *m*/*z* calcd for $C_{34}H_{58}Cl_3N_4O_4P_4Pd_4$ $(M - C1)^+$: 1245.8628, found: 1244.8888.

Synthesis of [{((μ-N(ᵗBu)P)$_2$)$_2$(μ-C$_6$H$_2$O$_4$)}{AuCl}$_4$] (16)

To a stirred solution of $AuCl(SMe_2)$ (0.032 g, 0.109 mmol) in dichloromethane (5 mL) was added dropwise a solution of **2** (0.015 g, 0.027 mmol) also in dichloromethane (6 mL), and the reaction mixture was stirred at room temperature for 4 h. The solution was concentrated to a small bulk and diluted with 1 mL of hexane and stored at room temperature for 24 h to give **16** as white crystalline solid. Yield: 86% (0.035 g). Mp: 153–157 °C (dec.). $C_{22}H_{38}N_4O_4P_4Au_4Cl_4$: C, 17.90; H, 2.59; N, 3.79. Found: C, 18.31; H, 2.37; N 3.43. ^{1}H NMR (500 MHz, $CDCl_3$) δ 7.42 (s, 2H, ArH), 1.44 (s, 36H, ᵗBu). $^{31}P\{^1H\}$ NMR (202 MHz, $CDCl_3$): δ 120.5 (s).

Crystal structure determination of compounds 2–8 and 15

A crystal of each of the compounds in the present work suitable for X-ray crystal analysis was mounted on a Cryoloop with a drop of Paratone oil and placed in the cold nitrogen stream on a Rigaku Saturn724 diffractometer or a Bruker APEX CCD (for **7**) diffractometer. Single crystal X-ray diffraction data collections were performed at 100–150 K using a Rigaku Saturn724 diffractometer with a graphite monochromated Mo-Kα radiation source (λ = 0.71073 Å) for compounds **2–6**, **8** and **15**. A Bruker Smart APEX CCD diffractometer with graphite monochromated Mo-Kα radiation was used for the data collection of compound **7**. The data were reduced using CrysalisPro Red 171.38.43 software. The structures were solved using Olex2[71] with the ShelXT[72] structure solution program using intrinsic phasing and refined with the ShelXL[73] refinement package using least squares minimization. All non-hydrogen atoms were refined anisotropically. Hydrogen atoms were placed in calculated positions and included as riding contributions with isotropic displacement parameters tied to those of the attached non-hydrogen atoms. In compound **2**, the large solvent void was SQUEEZED using PLATON.[74] The details of X-ray structural determinations are given in Tables 5 and 6, and bond lengths and bond angles are given in Tables 1–3. The powder X-ray diffraction (PXRD) was carried out on a EMPYREAN, Malvern Panalytical diffractometer with Cu-Kα radiation (λ = 1.54184 Å). Data were collected in a rectangular sample holder of dimension of Vol. 0.6 cm^3, *i.e.* l = 2, b = 1.5, h = 0.2 cm, at 298 K using a scan range (2θ/°) 5 to 100. Crystallographic data for the structures reported in this paper have been deposited with the Cambridge Crystallographic Data Centre as supplementary publication numbers CCDC 1883215 (compound **2**), 1883216 (compound **3**), 1883217 (compound **4**), 1883218 (compound **5**), 1883219 (compound **6**), 1883220 (compound **7**), 1883221 (compound **8**), and 1883222 (compound **15**).‡

Conflicts of interest

There are no conflicts to declare.

Acknowledgements

We are grateful to the Science & Engineering Research Board, New Delhi, for the financial support for this work. We also thank the Department of Chemistry, Indian Institute of Technology Bombay, Mumbai, for instrumentation facilities and for spectral and analytical data. M. K. P. thanks UGC, New Delhi, for SRF fellowship, H. S. K. thanks IITB for a fellowship, G. S. A. thanks CSIR, New Delhi, for SRF fellowship. J. T. Mague thanks the Louisiana Board of Regents for the purchase of the APEX CCD diffractometer, is thankful for an NSF-MRI grant No. 1228232 for the purchase of the D8 VENTURE diffractometer and thanks the Chemistry Department of Tulane University for the support of the X-ray laboratory.

References

1 M. S. Balakrishna, *Dalton Trans.*, 2016, **45**, 12252–12282.
2 M. S. Balakrishna, V. S. Reddy, S. S. Krishnamurthy, J. F. Nixon and J. C. T. R. B. S. Laurent, *Coord. Chem. Rev.*, 1994, **129**, 1–90.
3 M. S. Balakrishna, D. J. Eisler and T. Chivers, *Chem. Soc. Rev.*, 2007, **36**, 650–664.
4 L. Stahl, *Coord. Chem. Rev.*, 2000, **210**, 203–250.
5 G. G. Briand, T. Chivers and M. Krahn, *Coord. Chem. Rev.*, 2002, **233–234**, 237–254.
6 A. J. Plajer, K. Bold, F. J. Rizzuto, R. García-Rodríguez, T. K. Ronson and D. S. Wright, *Dalton Trans.*, 2017, **46**, 12775–12779.
7 W. T. K. Chan, D. Eisler, F. Garcia, S. Gonzalez-Calera, M. McPartlin, J. V. Morey, R. E. Mulvey, S. Singh, A. Steiner and D. S. Wright, *Chem. Commun.*, 2008, 2251–2253.
8 H. Klare, S. Hanft, J. M. Neudörfl, N. E. Schlörer, A. Griesbeck and B. Goldfuss, *Chem. – Eur. J.*, 2014, **20**, 11847–11855.
9 F. F. Wolf, J.-M. Neudörfl and B. Goldfuss, *New J. Chem.*, 2018, **42**, 4854–4870.
10 T. Beweries, R. Kuzora, U. Rosenthal, A. Schulz and A. Villinger, *Angew. Chem., Int. Ed.*, 2011, **50**, 8974–8978.
11 A. Brückner, A. Hinz, J. B. Priebe, A. Schulz and A. Villinger, *Angew. Chem., Int. Ed.*, 2015, **54**, 7426–7430.
12 A. Hinz, A. Schulz and A. Villinger, *Chem. – Eur. J.*, 2014, **20**, 3913–3916.
13 A. Hinz, A. Schulz and A. Villinger, *Angew. Chem., Int. Ed.*, 2016, **55**, 12214–12218.
14 A. Hinz, A. Schulz and A. Villinger, *Chem. Commun.*, 2016, **52**, 6328–6331.
15 A. Schulz, *Dalton Trans.*, 2018, **47**, 12827–12837.
16 E. L. Doyle, L. Riera and D. S. Wright, *Eur. J. Inorg. Chem.*, 2003, **2003**, 3279–3289.
17 F. García, J. M. Goodman, R. A. Kowenicki, M. McPartlin, L. Riera, M. A. Silva, A. Wirsing and D. S. Wright, *Dalton Trans.*, 2005, 1764–1773.
18 S. G. Calera and D. S. Wright, *Dalton Trans.*, 2010, **39**, 5055–5065.
19 D. Bawari, B. Prashanth, S. Ravi, K. R. Shamasundar, S. Singh and D. S. Wright, *Chem. – Eur. J.*, 2016, **22**, 12027–12033.
20 D. Tan, Z. X. Ng, Y. Sim, R. Ganguly and F. García, *CrystEngComm*, 2018, **20**, 5998–6004.
21 H.-C. Niu, A. J. Plajer, R. Garcia-Rodriguez, S. Singh and D. S. Wright, *Chem. – Eur. J.*, 2018, **24**, 3073–3082.
22 P. Chandrasekaran, J. T. Mague and M. S. Balakrishna, *Organometallics*, 2005, **24**, 3780–3783.
23 P. Chandrasekaran, J. T. Mague and M. S. Balakrishna, *Inorg. Chem.*, 2005, **44**, 7925–7932.
24 P. Chandrasekaran, J. T. Mague and M. S. Balakrishna, *Dalton Trans.*, 2009, 5478–5486.
25 M. M. Siddiqui, J. T. Mague and M. S. Balakrishna, *Inorg. Chem.*, 2015, **54**, 1200–1202.

26 A. Bashall, E. L. Doyle, C. Tubb, S. J. Kidd, M. McPartlin, A. D. Woods and D. S. Wright, *Chem. Commun.*, 2001, **2001**, 2542–2543.
27 S. Gonzalez Calera, D. J. Eisler, J. M. Goodman, M. McPartlin, S. Singh and D. S. Wright, *Dalton Trans.*, 2009, 1293–1296.
28 M. Chakravarty, P. Kommana and K. C. K. Swamy, *Chem. Commun.*, 2005, 5396–5398.
29 P. Kommana and K. C. Kumara Swamy, *Inorg. Chem.*, 2000, **39**, 4384–4385.
30 H. Alexander, S. Axel and V. Alexander, *Angew. Chem., Int. Ed.*, 2015, **54**, 668–672.
31 A. Nordheider, T. Chivers, R. Thirumoorthi, I. Vargas-Baca and J. D. Woollins, *Chem. Commun.*, 2012, **48**, 6346–6348.
32 A. Nordheider, K. Hull, K. S. Athukorala Arachchige, A. M. Z. Slawin, J. D. Woollins, R. Thirumoorthi and T. Chivers, *Dalton Trans.*, 2015, **44**, 5338–5346.
33 A. Nordheider, K. Hüll, J. K. D. Prentis, K. S. Athukorala Arachchige, A. M. Z. Slawin, J. D. Woollins and T. Chivers, *Inorg. Chem.*, 2015, **54**, 3043–3054.
34 Y. X. Shi, R. Z. Liang, K. A. Martin, D. G. Star, J. Diaz, X. Y. Li, R. Ganguly and F. Garcia, *Chem. Commun.*, 2015, **51**, 16468–16471.
35 M. E. Otang, D. Josephson, T. Duppong and L. Stahl, *Dalton Trans.*, 2018, **47**, 11625–11635.
36 A. J. Plajer, H.-C. Niu, F. J. Rizzuto and D. S. Wright, *Dalton Trans.*, 2018, **47**, 6675–6678.
37 R. Sevilla, R. J. Less, R. García-Rodríguez, A. D. Bond and D. S. Wright, *Dalton Trans.*, 2016, **45**, 1868–1871.
38 C. G. M. Benson, V. Vasilenko, R. García-Rodríguez, A. D. Bond, S. González Calera, L. H. Gade and D. S. Wright, *Dalton Trans.*, 2015, **44**, 14242–14247.
39 Y. X. Shi, K. A. Martin, R. Z. Liang, D. G. Star, Y. Li, R. Ganguly, Y. Sim, D. Tan, J. Díaz and F. García, *Inorg. Chem.*, 2018, **57**, 10993–11004.
40 Y. Sim, Y. X. Shi, R. Ganguly, Y. Li and F. García, *Chem. – Eur. J.*, 2017, **23**, 11279–11285.
41 P. Chandrasekaran, J. T. Mague and M. S. Balakrishna, *Inorg. Chem.*, 2006, **45**, 6678–6683.
42 P. Chandrasekaran, J. T. Mague and M. S. Balakrishna, *Dalton Trans.*, 2007, 2957–2962.
43 M. M. Siddiqui, J. T. Mague and M. S. Balakrishna, *Inorg. Chem.*, 2015, **54**, 6063–6065.
44 G. S. Ananthnag, S. Kuntavalli, J. T. Mague and M. S. Balakrishna, *Inorg. Chem.*, 2012, **51**, 5919–5930.
45 D. Suresh, M. S. Balakrishna and J. T. Mague, *Dalton Trans.*, 2008, 3272–3274.
46 M. M. Siddiqui, S. M. Mobin, I. Senkovska, S. Kaskel and M. S. Balakrishna, *Chem. Commun.*, 2014, **50**, 12273–12276.
47 Y. X. Shi, K. Xu, J. K. Clegg, R. Ganguly, H. Hirao, T. Friščić and F. García, *Angew. Chem., Int. Ed.*, 2016, **55**, 12736–12740.
48 Y. Sim, D. Tan, R. Ganguly, Y. Li and F. García, *Chem. Commun.*, 2018, **54**, 6800–6803.
49 M. S. Balakrishna, R. Venkateswaran and J. T. Mague, *Inorg. Chem.*, 2009, **48**, 1398–1406.
50 M. K. Pandey, J. T. Mague and M. S. Balakrishna, *Inorg. Chem.*, 2018, **57**, 7468–7480.
51 M. S. Balakrishna and J. T. Mague, *Organometallics*, 2007, **26**, 4677–4679.
52 G. S. Ananthnag, J. T. Mague and M. S. Balakrishna, *Dalton Trans.*, 2015, **44**, 3785–3793.
53 Y. X. Shi, R. Z. Liang, K. A. Martin, N. Weston, S. Gonzalez-Calera, R. Ganguly, Y. Li, Y. Lu, A. J. M. Ribeiro, M. J. Ramos, P. A. Fernandes and F. García, *Inorg. Chem.*, 2015, **54**, 6423–6432.
54 S. Ramdeehul, L. Barloy, J. A. Osborn, A. De Cian and J. Fischer, *Organometallics*, 1996, **15**, 5442–5444.
55 H. Werner and A. Kühn, *Angew. Chem., Int. Ed. Engl.*, 1979, **18**, 416–417.
56 M. M. Siddiqui, S. M. Mobin, J. T. Mague and M. S. Balakrishna, *Polyhedron*, 2015, **101**, 179–184.
57 R. Keat and D. G. Thompson, *J. Chem. Soc., Dalton Trans.*, 1978, 634–638.
58 R. Keat, D. S. Rycroft and D. G. Thompson, *J. Chem. Soc., Dalton Trans.*, 1979, 1224–1230.
59 R. Jefferson, J. F. Nixon, T. M. Painter, R. Keat and L. Stobbs, *J. Chem. Soc., Dalton Trans.*, 1973, 1414–1419.
60 D. Bawari, B. Prashanth, K. Jaiswal, A. R. Choudhury and S. Singh, *Eur. J. Inorg. Chem.*, 2017, **2017**, 4123–4130.
61 G. S. Ananthnag, J. T. Mague and M. S. Balakrishna, *J. Chem. Sci.*, 2015, **127**, 979–986.
62 G. S. Ananthnag, J. T. Mague and M. S. Balakrishna, *J. Organomet. Chem.*, 2015, **779**, 45–54.
63 M. S. Balakrishna and S. S. Krishnamurthy, *J. Organomet. Chem.*, 1992, **424**, 243–251.
64 P. Chandrasekaran, J. T. Mague, R. Venkateswaran and M. S. Balakrishna, *Eur. J. Inorg. Chem.*, 2007, **2007**, 4988–4997.
65 M. M. Siddiqui, J. T. Mague and M. S. Balakrishna, *J. Organomet. Chem.*, 2015, **794**, 81–87.
66 B. S. Furniss, A. J. Hannaford, P. W. G. Smith and A. R. Tatchell, *Vogel's Textbook of Practical Organic Chemistry*, 1989, 428–429.
67 M. A. Bennett, T. N. Huang, T. W. Matheson, A. K. Smith, S. Ittel and W. Nickerson, *Inorg. Synth.*, 1982, **21**, 74–78.
68 Y. Tatsuno, T. Yoshida, S. Otsuka, N. Al-Salem and B. L. Shaw, *Inorg. Synth.*, 1990, **28**, 342–345.
69 M.-C. Brandys, M. C. Jennings and R. J. Puddephatt, *J. Chem. Soc., Dalton Trans.*, 2000, **2000**, 4601–4606.
70 G. Giordano, R. H. Crabtree, R. M. Heintz, D. Forster and D. E. Morris, *Inorg. Synth.*, 1990, **28**, 88–90.
71 O. V. Dolomanov, L. J. Bourhis, R. J. Gildea, J. A. K. Howard and H. Puschmann, *J. Appl. Crystallogr.*, 2009, **42**, 339–341.
72 G. M. Sheldrick, *Acta Crystallogr.*, 2015, **71**, 3–8.
73 G. W. Sheldrick, *Acta Crystallogr., Sect. A: Found. Crystallogr.*, 2008, **A64**, 112.
74 A. Spek, *J. Appl. Crystallogr.*, 2003, **36**, 7–13.